ANBUL TECHNICAL UNIVERSITY ★ INSTITUTE OF SCIENCE AND TECHNOLOGY

PROCESSING OF AlN - B_4C / Al COMPOSITES

M.Sc THESIS

Engineer Menderes ÇIRAKOĞLU

Date of Submission : 24 AUGUST 1994

Date of Approval : 26 AUGUST 1994

Examination Committe

Supervisor : Prof. Dr. Adnan TEKİN

Member : Prof. Dr. Okan ADDEMİR

Member : Prof. Dr. Niyazi ERUSLU

AUGUST 1994

İSTANBUL TEKNİK ÜNİVERSİTESİ ★ FEN BİLİMLERİ ENSTİTÜSÜ

AlN - B_4C / Al KOMPOZİTLERİNİN ÜRETİMİ

YÜKSEK LİSANS TEZİ

Met. Müh. Menderes ÇIRAKOĞLU

Tezin Enstitüye Verildiği Tarih : 24 AĞUSTOS 1994

Tezin Savunulduğu Tarih : 26 AĞUSTOS 1994

Tez Danışmanı : Prof. Dr. Adnan TEKİN

Diğer Jüri Üyeleri : Prof. Dr. Okan ADDEMİR

: Prof. Dr. Niyazi ERUSLU

AĞUSTOS 1994

ACKNOWLEDGEMENT

I would like to thank Prof. Dr. Adnan TEKİN, my thesis advisor, for his support and contributions during the preparation of this thesis. I also gratefully acknowledge to Dr. Çetin TOY for his guidance and helpful comments and also to Dr. Erol METİN for valuable discussions. I wish to express my appreciation to Hüseyin SEZER for SEM studies. I also would like to thank Prof. William D. SCOTT of University of Washington for his valuable suggestions and contributions and Prof. O.J. WHITTEMORE of University of Washington for mercury porosimetry instructions. Some of the porosimetry analysis and optical microscopy studies were done at the Marmara Research Center, Gebze, therefore I would like to thank Dr. Tarìk BAYKARA head of Materials Department and researcher Yüksel PALACI for his assistance.

This study was carried out with the support of the United Nations Industrial Development Organization (UNIDO) and are gratefully acknowledged.

AUGUST, 1994 Menderes ÇIRAKOGLU, B.S.

CONTENTS

SUMMARY

Metal matrix composites are attractive engineering materials. They have good properties like; high strength, low weight, higher service temperature and higher elastic modulus. There are several methods for the preparation of these composites. Infiltration is one of the most economical process. Infiltartion can be done by two ways; by pressure and by wetting assisted. Wetting assisted infiltartion becomes important when near net shape composites are needed. Many metals have been considered as a possible matrix material. Copper, titanium, magnesium and aluminum. Aluminum matrix composites are more widely used at present.

In this study, AlN - B_4C ceramic preforms were infiltrated with aluminum metal. To understand the effect of B_4C to infiltration, preforms contains different percentage of B_4C (1, 2, 4 and 10 wt%) were prepared. The mixtures first dry pressed then cold isostatically pressed at 25000 psi. Then sintered at 1400-1600°C for 1 hour under nitrogen flow in an induction furnace. 99.99% pure aluminum metal was used for infiltration. Infiltration experiments were carried out in the same furnace by placing the aluminum metal into the reservoir of cup shaped sintered preforms. Heating was conducted under vacuum to 900°C.Infiltration experiments were done under different atmosphere (50 torr, 400 torr and vacuum). The infiltration temperature was 1250°C.

Each sample was weighed before and after every sintering experiment to determine weight change. Infiltrated samples were cut through the middle, mounted and polished for optical microscopy. Pore distribution of the sintered preforms were analyzed by mercury porosimetry and surface area measurements were done by 3 point BET method. Hardness of the composites were measured with macro Vickers.

Weight change measurements showed that, for a succesful infiltration for this system samples must weight gain which indicates the reduction of Al_2O_3 on AlN surface. Pore analysis indicated that, pore size decreases with increasing B_4C content. Higher hardness values are obtained from the samples which have higher ceramic content.

AlN-B_4C KOMPOZİTLERİNİN ÜRETİMİ

ÖZET

Sermet olarak isimlendirilen seramik- metal kompozitleri, her iki malzemenin iyi fiziksel ve mekanik özelliklerini biraraya getirdigi için bir mühendislik malzemesi olarak çok önemlidir. Özellikler, bileşenlerin kompozit içindeki miktarlarını değiştirerek modifiye edilebilir.

Metal matrixli kompozit malzemeler konusundaki araştırmalar 20 yıldan daha uzun bir zamandır devam etmektedir. Bu araştırmalar yeni malzemelerin geliştirilmesi zorunluluğundan doğmuştur. Yeni malzeme geliştirilmesinde birbiriyle çelişkili gibi görünen iki önemli parametre göz önünde bulundurulur, bunlar yüksek performans ve düşük maliyettir. Bu iki faktör, farklı malzemelerin biraraya getirildiği kompozit malzemelerin geliştirilmesine yol açmıştır. Metal matrixli kompozit malzemeler yüksek mukavemet, hafif ağırlık, yüksek aşınma direnci, elastik modül gibi önemli özelliklere sahiptirler.

Seramik-metal kompozitlerin üretimi konusunda literatürde çeşitli yöntemler önerilmektedir. Bu metotlar başlıca 5 kısma ayrılabilir: Difüzyon bağlanması, ön karıştırılmış sulu karışımların basıçlı veya basınçsız katılaştırma dökümü, bir sıvı fazın preform içerisine basınç yardımıyla veya ıslatma yardımıyla infiltrasyonu ve ön karıştırılmış seramik-metal tozlarının ıslatma koşulları sağlanarak sinterlenmesi. Tabakalı kompozit yapıları için en uygun teknik difüzyon bağlanması yöntemidir. Bu yöntemde, matrix ve fiber tabakaları istenen şekilde üst üste dizilir daha sonra matrix malzemesinin ergime sıcaklığının altındaki bir sıcaklıkta sinterlenir. Bu yöntemle üretilen kompozitlerde özellikler anisotropiktir. Metal-seramik partikül kompozitlerinin katılaştırma dökümü ile üretiminde, seçilmiş erimiş haldeki bir matrix malzemesi içine seramik partiküller katılarak dispersiyon sağlanır. Daha sonra bu karışım, uygun dağılımı sağlayabilecek uygun koşullar altında katılaştırılır. Bu yöntem yaygın olmasına rağmen, matrix fazında segregasyon, kalıcı porozite ve çekilme gibi problemler görülür. Ayrıca, katılaşma sırasında oluşan mikrosegregasyonlar, kompozitin mekanik özelliklerini olumsuz olarak etkiler.

İnfiltrasyon bu yöntemler içinde en ekonomik ve çok yönlü uygulama alanı bulan bir yöntemdir. İnfiltrasyon sırasında ergimiş metal seramik malzemedeki gözenekleri doldurarak bir kompozit malzeme oluşturulur. Sıvı faz sintetlemsine benzemekle birlikte infiltrasyonda sıvı haldeki metal ile gözenekli seramik diştan temastadırlar ve sıvı gözenekleri kapiler kuvvetle doldurur. Bu yöntemle, ek bazı işlemlere (extrüzyon, sıcak presleme v.b.) yüksek yoğunluklu malzemeler üretilebilir. Ayrıca karmaşık şekilli veya büyük boyutlu ürünler istenen nihai şekle çok yakın olarak üretilebilir. Islatma olayında olduğu gibi, infiltrasyon içinde önemli bir koşul sıvı metal ile seramik faz arasındaki temas açısının düşük olmasıdır. Bunun dışında başarılı bir infiltrasyon için aşağıdaki koşullar da önemlidir:

* Çeşitli yöntemlerle şekillendirilmiş seramik toz, kapiler kuvvetle infiltrasyonu sağlayacak şekilde por boyutu ve dağılımına sahip olmalıdır.

* Metal fazın ergime sıcaklığı, seramik malzemenin ergime sıcaklığından düşük olmalı ve sıvı halde akışkanlığı yüksek olamlıdır. Metalin ısıl genleşme özellikleri, infiltre olmuş numunenin nihai mukavemetini önemli ölçüde etkiler. Eğer katılaşma sırasında sıvı haldeki metal genleşirse kompozitin mukavemeti azalır.

* Sıvı metal faz ile seramikfaz arasındaki reaksiyon az olmalıdır. Çünkü eğer infiltrasyon sırasında oluşan reaksiyon ürünlerinin hacmi, başlangıçtaki seramik ve sıvı metalin hacimlerine eşit veya daha büyük olursa, sıvı metal gözenekleri tamamen dolduramaz ve infiltrasyon tamamlanamaz.

* Searmik fazın metal içindeki çözünürlüğü az olmalıdır, aksi durumda infiltrasyon hızı azalır.

* İnfiltrayon sistemine vakum uygulanması, kapiler infiltrasyonu arttırabilir.

* B_4C/ Al ve SiC/ Al gibi infiltrasyon sırasında kuvvetli kimyasal reaksiyonların meydana geldiği sistemlerde infiltrasyon basınç uygulanarak gerçekleştirilebilir. Basınç uygulaması ile infiltrasyon sıcaklığı düşürülerek sıvı metal ile searmik fazları arasındaki reaksiyonlar azaltılır. Ayrıca sıvı metalin seramik fazı ıslatmasının az olduğu veya por boyutu ve dağılımı uygun olmayan sistemlerde de yeterli basınç uygulaması ile üretilebilecek parçaların boyutları sınırlıdır ve işlem sırasında seramik fiberlerin zarar görmesi söz konusudur. Basınçlı infiltrasyonun en önemli

dezavantajı, ergimiş metalin üzerine basınç uygulayabilmek için alet ve donatımın gerekli olmasıdır.

İnfiltrasyon yönteminin geliştirilmesi sırasında çeşitli metotlar denenmiştir. Kısmen daldırarak yapılan infiltrasyonda, seramik parça ergimiş metal banyosu içine kısmen daldrılır, kapiler kuvvetin etkisiyle sıvı gözenekleri doldurur. Tam doldurmalı infiltrasyonda seramik parça ergimiş metal içine tamamen daldırılır ve sıvı her yönden gözenekleri doldurur. Diğer bir metotda başlangıçta seramik ve metal birbirleriyle temas edecek şekilde yerleştirilir ve yüksek sıcaklıklara çıkıldığında metal ergiyerek seramik malzemedeki gözenekleri doldurur.

Bu çalışmada alüminyum metali ile infiltre edilmek üzere AlN ve B_4C içeren seramik preformlar hazırlanmıştır. Alüminyum nitrür kovalent bağa sahip ve önemli özellikleri olan bir nitrür seramiktir. En dikkat çekici özelliği yüksek ısıl iletkenliğidir. AlN tek kristalin oda sıcaklığındaki ısıl iletkenliği 320 W/mK dır. Polikristalin AlN ün ise üretim şartları ve saflığa bağlı olarak 10-260 W/mK arasında değişir. AlN ün içerdiği empüriteler özellikle oksijen atomları AlN kafes içinde çözünerek ısıl iletkenliği düşürür. Yüksek ısıl iletkenliğinin yanı sıra düşük ısıl genleşme katsayısına sahiptir ayrıca iyi bir yalıtkandır. Karbon monoksitli ortamda 1800°C ye, hidrojenli ortamda 1400°C ye, vakum altında 1500°C ye ve azot atmosferinde 2700°C ye kadar kararlıdır. Oksitleyici ortamlara karşı oldukça hassastır, 1000°C nin üzerindeki sıcaklıklarda AlN ün Al2O3 e oksidasyonu oldukça hızlıdır bu nedenle yüksek sıcaklıklarda oksitleyici atmosferde uygulama alanı kısıtlıdır.

Saf alüminyum nitrürü klasik yöntemlerle sinterlemk mümkün değildir. Her ne kadar, ticari AlN ü 2000°C de sıcak presleme ile sinterleyerek teorik yoğunluğun % 97-99 una sahip malzemeler üretmek mümkünse de bu yöntemle sadece basit şekilli parçaların üretilebilmesi ve pahalı olması araştırmacıları basınçsız sinterleme konusuna yöneltmiştir. Yapılan çalışmalar periyodik tablonun ikinci ve üçüncü grup elemntlerinin oxitlerinin sinterlemeye olumlu katkılarının olduğunu ortaya koymuştur.

Bu çalışmada AlN ile birlikte kullanılan ikinci seramik malzeme B_4C dür. Düşük yoğunluk (2.52 gr/ cc), yüksek sertlik (Mohs skalasında 9.5) gibi özelliklere

sahip olması dolayısıyla aşınma direnci ve darbe direnci gerektiren uygulamalar için uygun bir malzemedir. Gevrek kırılganlığı en önemli dezavantajıdır. AlN gibi B_4C de sinterlemek zordur. Yüksek sıcaklıklarda (2100°C) sıcak presleyerek yüksek yoğunluklar elde edilebilir. Bor karbürü metalik bir malzeme ile kompozit yaparak mekanik özellikleri geliştirilebilir. Halverson ve arkadaşları kolay bulunabilmesi, toksik olmaması, sünek olması ve nispeten ucuz olması sebebiyle alüminyum metalini kullanmışlardır.

İnfiltrasyon için ıslatma olayı önemli bir parametre olduğu için kullanılacak malzemelerin metal matrix ile (bu çalışmada alüminyum) ıslanabilirliği konusunu bilmek önemlidir. AlN, alüminyum ile süblimasyon sıcaklığı olan 2800°C ye kadar reaksiyona girmez. Bu nedenle AlN/Al kompoziti termodinamik olarak kararlıdır ve zararlı olabilecek reaksiyon ürünleri meydana gelmez. Rhee'nin çeşitli seramik malzemelerin alüminyum ile ıslanmaları konusundaki çalışmalarına göre, AlN/Al sistemi en az ıslanma gösteren sistemdir. Bununla birlikte, 1000°C nin üzerinde vakum altında alüminyum B_4C ü ıslatmaya başlar ve B_4C ile alüminyum arasındaki kimyasal reaksiyonlar sonucu birçok ikili ve üçlü bileşik oluşur. Bu reaksiyonlar sistemin yüzey enerjisinin sürekli değişmesine neden olur bu da serbest enerjinin azalmasına ve bunun sonucu olarak alüminyumun B_4C üzerinde yayılmasına sebep olur.

Bu çalışmada alüminyum ile etkileşimi farklı olan iki seramik malzeme çeşitli oranlarda karıştırılarak, alüminyum metali ile infiltrasyonu denenmiştir. Bor karbürün seramik preformdaki miktarına bağlı olarak infiltrasyonu nasıl etkilediği incelenmiştir.

Ticari AlN (Hermann Starck , ortalama partikül boyutu 13.6μ) ve B_4C (ESK, ortalama partikül boyutu 5μ) tozları kullanılmıştır. Tozlar, AlN ün suya karşı reaktif olamsı dolayısıyla isopropanol alkol içinde, karışımdaki B_4C ün ağırlıkça yüzdesi sırayla 1,2,4 ve 10 olacak şekilde hazırlanmıştır. Karıştırma işlemleri önce mekanik daha sonra ultrasonik karıştşrıcı kullanılarak yapılmıştır. Ultrasonik karıştırma sırasında karışıma ağırlıkça %4 bağlayıcı (Carbowax 8000, polietilen glikol) katılarak numunelere mukavemet kazandırılmıştır. Hazırlanan tozlar, çelik bir kalıba belirli miktarda doldurularak,kuru presleyici ile eşeksenli olarak 1800 kg lık yük altında şekillendirilmiştir. Daha sonra soğuk isostatik pres ile 172 MPa basınç ile her yönden sıkıştırılmıştır. Bağlayıcı

uçurma işlemi 200°C de 1 saat tutularak yapılmıştır. Hazırlanan seramik preformlar 1400-1600°C de azot altında 1 saat sinterlenmiştir. Sinterleme fırını olarak bir indüksiyon fırını kullanılmıştır. İnfiltrasyon işlemleri de aynı fırın da gerçekleştirilmiştir. % 99.99 saflikta alüminyum numuneleri sinterlenen kap şekilli numuneler üzerine yerleştirilerek 1250°C de yapılmıştır. İnfiltrasyon işlemi vakum, 50 torr ve 400 torr Ar gibi çeşitli ortamlarda gerçekleştirilmiştir. Kullanılan argon gazı sisteme bakır ve titanyum dan geçirilip temiz bir şekilde verilmiştir.

İnfiltrasyon sonrası numuneler, elmas kesici ile kesilmiş ve çeşitli tane büyüklüğüne sahip SiC aşındırıcı kağıtlar ve alümina solüsyonu kullanılarak çuha üzerinde parlatılmıştır.

Genellikle nitrürler bir miktar oksijen içerirler, AlN deki bu oksijen Al_2O_3 formundadir. Bilindiği gibi aluminyum oksit infiltrasyonu önlediği için uzaklaştırılması gereklidir. Karışımdaki B_4C un tüm Al_2O_3'u, AlN ve BN e dönüştürebilmesi için B_4C yüzdesinin %2 nin üzerinde olması gerektiği hesaplanmıştır. Ağirlık kazanımı meydana gelen numunelerde bu dönüşüm oluşmakta ve bu nedenle de infiltrasyon gerçekleşmektedir.

Civa porozimetresi analizleri, sinterleme sıcaklığının artışı ile por boyutunda artış gözlenmiştir, bu muhtemelen tanelerin sinterlenerek büyümesi sonucu oluşmaktadır.

İnfiltre olan numunelerin X-ışınları ile analizlerinde tam infiltre olmuş numunelerde yarı infiltre olmuş olanlara göre daha şiddetli Al piklerine rastlanmıştır.

Kompozitlerin sertlik ölçümleri, makro Vickers cihazı ile 50 kg lık yük kullanılarak yapılmıştır. B_4C yüzdesinin artışı ile sertlikte artış olduğu bulunmuştur ayrıca 50 torr ve 400 torr da yapılan deneyler sonucu elde edilen kompozitlerin sertligi vakumda üretilenlere göre daha düşük çıkmaktadır. Bunun sebebi olarak, ergimiş metalin vakum altında daha kolay hareket etmesi ve ayrıca argon basıncı altında, preformdaki gözenekler gaz ile dolu olacağından ergimiş metalin gözenekleri doldurmasına imkan vermeyeceği düşünülmüştür.

CHAPTER 1. INTRODUCTION

Metal- ceramic composites are one of the most attractive engineering materials. There have been an intense research on these materials for more than twenty years [1]. There are two important requirements for developing new materials; these are improved performance and a reduction in material cost. For example, in aerospace applications, the dominant requirement is the reduction in stuructural weight [2]. Metal - ceramic composites have good properties like high strength, low weight, higher service temperature, high elastic modulus [3].

There are four reinforcement phases for metal - matrix composites; these are particles, whiskers, discontinuous and continuous fibers [4]. Many particle reinforced composites have been used in industry for many years. Particles strengthen and stiffen the matrix metal by preventing movement of dislocations in the metal's crystal lattice. Particle reinforced composites include cermets used in the electronics industry for the tracks of precision variable resistors and tungsten carbide in cobalt for high speed tool tips. SiC particulate reinforced aluminum is also being investigated in automotive industry for such applications as brakes, pistons and valves. And also this material has desirable properties such as lightweight, good thermal conductivity and tailorable coefficient of thermal expansion (CTE) [5]. Particulate reinforced aluminum alloys have spesific stiffnesses and substituting the landing skids of a helicopter by particulate reinforced aluminum have been evaluated and significant weight savings with no loss in performance were achieved and also wear resistance was

increased [2]. Particulate reinforced aluminum tennis rackets and golf club heads were also produced.

Whiskers are single crystals with high length to diameter ratio. The major whisker material is SiC [4]. Currently, aluminum parts reinforced with SiC whiskers are being fabricated and tested for several automotive applications. These parts are referred to as discontinuously reinforced aluminum (DRA) and they are a subclass of metal matrix composites. DRAs are a combination of high strength aluminum alloys reinforced with either SiC whiskers, fibers or particles. Whisker reinforced parts have some advantages, they are easier to fabricate, their cost is less than fiber reinforced parts and they provide isotropic property improvements [6].

The most common discontinuous fibers are alumina and alumina - silica. These fibers are usually woven together like blankets of insulation. They may be compacted into a preform to be used for local reinforcement. Boron, silicon carbide and graphite fibers give their high tensile strength, high stiffness and low coefficient of thermal expansion to the matrix metal [4]. SiC is the most common fiber at the present time and it must be coated because the reactivity with oxidizing environments [5]. Metal matrix composites attracted commercial attention in 1983 when Toyota Motor Corp. started using composite pistons in diesel engines. Art Metals Co. of Japan are currently manufacturing over 100000 reinforced pistons per month for Toyota car diesel engines. This application has resulted in no additional cost. Honda have produced a stainless steel wire reinforced aluminum conrod for one of its cars, a 30% weight saving was achieved with improvements in engine power and fuel economy. The first application of metal matrix composites was for the space shuttle. Struts made of boron fibre

reinforced aluminum composites are lightweight and have high stiffness struts made of boron fibre reinforced aluminum composite. Use of this composite allowed smaller tube diameters and since the composite has low thermal conductivity, the amount of insulation required between the equipment and the skin was reduced. High modulus composites are being investigated for space satellite applications where high spesific stiffness and strength is required in combination with high dimensional stability. Other interesting application area of metal - matrix composites is sporting goods. Bicycle frames made of boron reinforced aluminum composites have been used at the Los Angeles olympic games [2].

In Table 1.1, potential metal matrix composites applications for the automotive industry are listed [6]. And in Table 1.2, the representative properties of metal - matrix composites are listed [4].

There are several methods for the preparation of ceramic - metal composites. These are; diffusion bonding, solidification casting of premix slurries with or without pressure, pressure assisted infiltration, wetting assisted infiltration and sintering of premix ceramic and metal powders under wetting conditions. Diffusion bonding is a common technique for laminated composites. In this method, several layers of matrix and fibers are laid up then sintered below the melting temperature of matrix material. In solidification casting, dispersoids are dispersed in a selected melt matrix material then this mixture is solidified. But there are several problems with this method, like residual porosity and shrinkage. Furthermore, microsegregation during the solidification process affect the mechanical properties of the composite adversely [7].

TABLE: 1.1. Metal - matrix composite applications for the automotive industry [6].

System	Component	MMC Properties
Engine	Piston crown	High temperature, fatigue, creep, wear resistance
	Valve	High temperature, fatigue, creep,wear
	Connecting rod	Increased stiffness, weight reduction
Suspensions	Struts	Damping, increased stiffness
Driveline	Shift forks	Wear resistance, weight reduction
	Gears	Wear resistance, weight reduction
	Wheels	Weight reduction
Brakes	Disk rotors	Wear resistance, weight reduction
	Calipers	Wear resistance, weight reduction

TABLE: 1.2. Representative properties of metal matrix composites [4].

Matrix	Reinforcement	Reinforcement (Vol %)	Modulus(10^6psi)	
			Longi tudinal	Trans verse
Al	None	0	10	10
Epoxy	High strength graphite fibers	60	21	15
Al	Alumina fibers	50	29	22
Al	Boron fibers	50	29	18
Al	Ultrahigh modulus graphite fibers	45	50	5
Al	Silicon carbide particles	40	21	21
Ti	Silicon carbide monofilament fibers	35	31	24

Infiltration is one of the most economical process for the production of composites having a matrix of low (or medium) melting point metals such as aluminum, magnesium or copper [8]. Pressure assisted infiltration is good for incompatible composites such as B_4C-Al and SiC-Al where strong chemical reactions exist during infiltration. The application of pressure permits lowering the infiltration temperatures to reduce chemical reactions between the matrix and ceramic. But this method limits the sizes and shapes that can be produced. Wetting assisted infiltration does not require external pressure

and also reduces the residual porosity. This method becomes important when near net shape cermet productions are needed. There are several requirements for a succesful pressureless infiltration; the presence of open porosity throughout the microstructure, good wetting of the ceramic by molten metal, chemical interactions between the constituents during infiltration [7].

Many metals have been considered as a possible matrix material; aluminum, copper, titanium, magnesium, zinc, nickel etc.

* **Copper:** Although copper is heavier than aluminum and titanium, it is an excellent conductor for both heat and electricity and also its shear strength is higher than aluminum at temperatures above 400°C. Copper is relatively inert to reinforcing materials and therefore it has fewer manufacturing problems than titanium [4].

* **Titanium:** Another lightweight metal and it is getting much attention in composites research. But it has some disadventages like the cost is higher, applications are more specialized [4].

* **Magnesium:** It is lighter than aluminum and especially suitable as a composite matrix because of its natural tendency to wet the filler [4].

* **Aluminum:** It is lightweight, nontoxic, relatively inexpensive, easy to obtain and it has low density, low electrical resistivity, high thermal conductivity making it an attractive matrix material for metal matrix composites. Aluminum - matrix composites are the most widely used at present [4,6,9].

In this study, aluminum is used as a matrix material. The purpose of this study is to investigate the processing parameters of AlN - B_4C / Al composites. And also to understand the effect of B_4C and different atmospheres to infiltration.

CHAPTER 2. BACKGROUND INFORMATION

The most important requirement for the fabrication of metal - matrix composites (especially by processes involving liquid metals) is wetting of the ceramic phase by molten metals [10]. Good wetting is a requirement for satisfactory bonding between solid ceramic phase and liquid metal matrix phase [11]. Therefore, understanding of wetting becomes an important subject to study.

2.1. Interface energy and interface tension

The atoms or molecules at or near the surface are attracted inwards and sideways due to presence of neighbor atoms in those directions. Compared to atoms located within bulk part of material, forces on an atom located on the surface are not balanced. This means that work has to be done in order to bring a molecule from the bulk to the surface. Bringing an interior atom to the surface requires work to be done which results in an increase in free energy Surface energy is then defined as the increase in free energy per unit area of new surface formed (J/ m^2). The total free energy of a material under constant temperature and pressure can be expressed as shown below;

$$G = G_0 + \gamma A \qquad (2.1.)$$

where

γ: Excess free energy per unit area

A: Surface area

G_0: Bulk free energy of the system

Since bulk free energy is constant, change in the system free energy under fixed pressure and temperature is

due to the presence of surface.

$$dG = \gamma dA + Ad\gamma \qquad (2.2)$$

If one considers a classical example of a soap film being pulled along a wire frame under applied force F, work performed will be equal to FdA where dA is the increase in area. According to definition of surface free energy, this work should be equal to the amount of free energy change.

$$dG = FdA = \gamma dA + Ad\gamma \qquad (2.3)$$

$$F = \gamma + A \frac{d\gamma}{dA} \qquad (2.4.)$$

In the case of liquids, the molecules are mobile enough as to be able to the imbalance of forces acting on them in the surface layer so it can keep a constant surface structure, and $d\gamma / dA$ is equal to zero. Therefore;

$$F = \gamma \qquad (2.5.)$$

Equation 2.5 for a liquid implies that surface tension is equivalent to surface free energy. For solids, it is not possible to say that $d\gamma / dA$ is equal to zero, because atoms can not rearrange themselves as easily as liquid atoms [1,7].

Various techniques have been introduced for determining the surface energy and wettability of liquids. Measurements of surface free energies of liquids are relatively easy compared to measurement of solid surface energies. For liquids, the most common methods

are the sessile drop, the pendant drop, maximum bubble pressure method and capillary rise methods. For solids, the only technique is the zero - creep method where a polycrystalline material is elongated at high temperature and the garin boundaries intersecting solid - vapor interface sustain equilibrium by the movement of atoms at the grain boundaries [7]. Sessile drop method is often used for measurement of surface energies of liquids. This method is advantageous, because it permits the determination of the contact angle of the liquid and surface energy at the same time [12]. Even though the wettability experiments are simple, the contact angle values reported in the literature for the same system shows a quite variation. This may be due to the sensitivity of contact angle and surface energy to the presence of impurities in the substrate and/or in the working atmosphere and to surface roughness of the substrate [13].

In Table 2.1. measured surface energy values of liquid aluminum is shown [7,14]. As it can be seen from this table, measured surface energy values of molten aluminum shows a wide variation. One possible reason of variation is due to the presence of oxide skin on the molten aluminum surface. Effects of alloying elements on surface energy of liquid aluminum is shown in Figure 2.1. some alloying elements can decrease, increase or some of them have no influence on the measured surface energy [7].

Absorption and/or reactions between solid, liquid and gas phases can result to some changes in solid, liquid and solid - liquid surface free energies. Since the measurement of solid and solid - liquid surface energies is difficult, it is desirable to develop theoretical techniques for approximate estimations.

Surface energy is the work to expand the surface area, therefore it is related to atomic bonding and parameters such as melting temperature, elastic modulus, hardness. These parameters can provide a rough estimate of surface energy. Some of the estimated and measured results for several ceramic materials are summarized in Table 2.2. [7].

TABLE: 2.1. Surface energy of pure molten aluminum [7].

Temperature (°K)	γ_{lv} (mJ/m^2)	$d\gamma/dT$	Temp. Range (°K)	Atmosphere
Al (oxidized surface)				
933	760	0.202	980-1090	10^{-7}
933	865	0.14	973-1473	10^{-5}
933	870	0.195	933-1293	10^{-6}
973	869	0.20	1073-1173	Ar+100ppm O_2
Al (unoxidized surface)				
973	1122	---	---	Ar

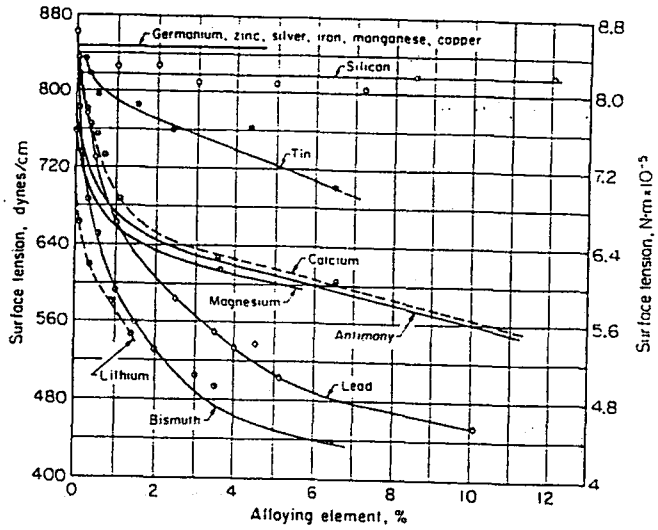

FIGURE: 2.1. Effect of alloying elements on the surface tension of 99.99 % Al at 700 to 740°C in argon [7].

TABLE: 2.2. Surface energies of some solid ceramics [7].

Material	Temperature (°K)	γ_{sv} (mJ / m^2)
Al_2O_3	2143	925
Al_2O_3	2123	905
MgO	1870	1100
MgO	0	1090
TiO_2	2100	380
SiC	1703	1850
ZrC	1373	800+/- 250
TiC	1373	1190+/- 350
WC	1423	2820+/- 30
AlN	1703	2470
Si_3N_4	1703	1150

2.2. Wetting Phenomena

The wettability of a solid by a liquid is indicated by the contact angle (θ) between the two phases. Figure 2.2 shows a liquid drop resting on a solid substrate, surrounded by a vapor phase.

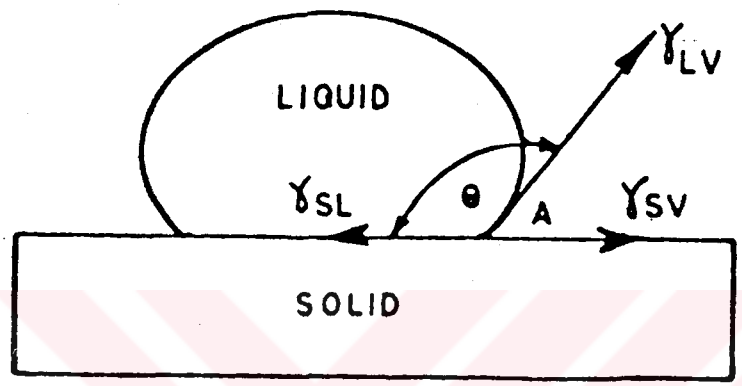

FIGURE: 2.2. Schematic diagram of a liquid drop resting on a solid surface [10]

For ideal wetting, the liquid drop must spread completely over the solid surface, in this case the contact angle becomes zero. Non- wettability is defined by the contact angle of 180°. However, a contact angle less than 90° cause effective wetting and a contact angle greater than 90° cause non - wetting [10]. In Figure 2.3, a liquid drop on the solid surface showing the wetting angle for wetting and non - wetting systems.

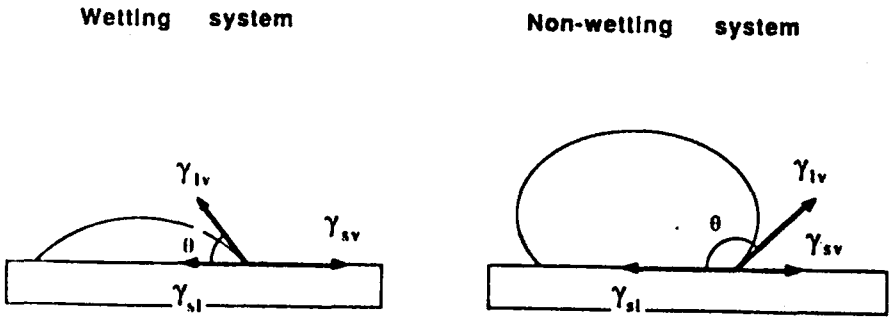

Figure: 2.3. Schematic diagram showing wetting and non- wetting systems [11].

The relationship between interface tensions and wetting angle is described by Young's equation [15].

$$\gamma_{sv} = \gamma_{sl} + \gamma_{lv} \text{ Cos } \theta \qquad (2.6.)$$

or

$$\text{Cos } \theta = \frac{\gamma_{sv} - \gamma_{sl}}{\gamma_{lv}} \qquad (2.7.)$$

where

γ_{sv} = Interface tension between solid - vapor

γ_{sl} = Interface tension between solid- liquid

γ_{lv} = Interface tension between liquid- vapor

θ = The angle between the liquid and substrate (contact angle or wetting angle)

A liquid wets the solid surface when $\gamma_{sv} - \gamma_{sl}$ is positive (Cos $\theta > 0$) [1]. The contact angle in Young's equation (equation 2.6) is defined for chemically homogeneous and perfectly smooth solid surfaces. Real solid surfaces never fulfill these conditions, therefore measured contact angles may deviate from Young's angle [13]. To increase the interaction between metal and ceramic phases, the surfaces have to be brought into excited states. Therefore, temperature and atmosphere are as important as the properties and structure of the surfaces. Work of adhesion (W_a) describes the physical interaction between a metal and a ceramic. The work of adhesion (W_a) is defined by Dupre's equation [12,16].

$$W_a = \gamma_{sv} + \gamma_{lv} - \gamma_{sl} \qquad (2.8.)$$

W_a also shows the strength of the binding between the two phases. It has dimensions of an energy per unit surface area [1].

Combining equations (2.6) and (2.8), the work of adhesion can be written as follows,

$$W_a = \gamma_{lv} (1 + \cos \theta) \qquad (2.9.)$$

When the surface energy of the liquid phase is (γ_{lv}) known, W_a can be determined from the measurement of contact angle [1].

The surface energies of ceramics (solids) are usually lower than that of pure metals (liquids). And this results in low values of ($\gamma_{sv} - \gamma_{sl}$) which is the driving force for wetting. According to equation 2.7, the contact angle between a liquid drop and solid can be decreased by:

* Increasing the surface energy of the solid (γ_{sv})
* Decreasing the interfacial energy between the solid and the liquid (γ_{sl})
* Decreasing the surface tension of the liquid (γ_{lv})

2.3. Mechanism of Wetting

Although the mechanism of wetting is not fully understood there are several theories about it. The main mechanisms for wetting between ceramic and liquid metal are; electronic charge transfer, dissolution, adsorption and chemical reactions [11].

*** Electronic Interaction :** It has been suggested that the interaction force between liquid metal phase and solid compound is determined by the electronic configuration of these two phases. Samsanov et al., studied the wetting of carbides with liquid metals. They explained the wetting behavior on the basis of

elements have strong affinity to oxygen. Therefore, adsortion of vaporized species on the solid phase is not believed as an active wetting mechanism for ceramic/Al-alloy system [11].

* **Interfacial Reaction :** Many researchers have suggested that interfacial reactions such as chemical reaction, dissolution and adsorption can make solid:liquid system wettable. In each case, the driving force is a reduction of total free energy of system. However, excessive reactions can cause degradation of solid phase or unwanted phase formation at the interfacial region [11].

Most solid ceramic:liquid metal systems are chemically inert, therefore the interfacial reaction may not be the major wetting mechanism. In this case, the first mechanism may be either electronic interaction or simply physical contact [11].

The stability of ceramic phases in ceramic:liquid metal systems permit only very low mutual solubilities between the two phases. However, small amounts of dissolution can decrease solid:liquid interfacial energy significantly [11].

2.4. Infiltration

There has been a considerable interest in the synthesis of metal - matrix composites using liquid metal infiltration techniques recently. However, the practice of infiltrating porous materials with molten metals is very old. It has been used since 1920's to strengthen powder metallurgy products made of iron and steel by infiltrating them with copper. It is the standart method of producing electrical contacts of tungsten and

molybdenum by infiltrating them with silver or copper. The method is not restricted with metals, for example; wood has been infiltrated with babbitt metal and bronzes have been infiltrated with oil [17,18].

During infiltration, a liquid metal moves through the pore system of a solid powder compact. Although it is similar to liquid phase sintering, in infiltration liquid externally contacts the porous solid and capillary forces draw it inward. Infiltration has some advantages over other techniques, these are as follows [19].

a) Full density can be obtained without application of high pressures or subsequent forging, rolling or extrusion or hot pressing.

b) Complex shapes and large sizes can be produced with a near net shape.

c) Surface characteristics that permit joining and coating can be obtained.

d) Phase distribution that may result in a uniform or a purposely graded microstructure can be obtained.

e) Good mechanical properties can be obtained. Strength can be increased through subsequent effective heat treatment.

For a succesful infiltration of a porous solid with a liquid phase, the total surface free energy of the system after infiltration must be lower than the total surface free energy before infiltration. Here the total means the surface free energies of the solid and the liquid phases as well as the interfacial energy between the solid and the liquid . This relationship is another form of equation 2.6 and is given below.

$$\gamma_{sl} = \gamma_{sv} - \gamma_{lv} \cos \theta \qquad (2.10)$$

Infiltration rate is related to Poisseuille's law which defines the rate of flow or rise of a liquid in a glass capillary. This model is based on the assumption that all capillaries are straight but in real powder compacts there may be twisted channels. Furthermore, in many systems after penetration, pore filling liquid reacts with the solid which is thought to be the second infiltration stage. Similar to wetting, low contact angle is also important for infiltration. Many conditions other than low contact angle must be fulfilled for a succesfull infiltration [19].

Powder compact: The compacted powder should contain interconnected pores and channels, and the size range of the pores must allow capillary force action. The type of the furnace must permit control of time and temperature for both stages of infiltration (penetration of the liquid through the pore system and reaction of the liquid with the powder compact after filling the pores). The particle size distribution of the powder and the compacting pressure must be adjusted so that to produce many interlocking pores free paths between them for to receive and pass the liquid metal [19].

Infiltrant: It must have a melting temperature below the melting point of ceramic solid. High fluidity in the liquid state is desirable, because it helps the driving force of the surface tension. Thermal expansion characteristics of the infiltrant affect final strength of the infiltrated sample. If the infiltrant, expands during rapid solidification, the strength of the composite may be decreased [19].

System Compatibility: As it was mentioned above, the wetting angle between the liquid infiltrant and the compacted powder should be low ($\theta < 90°$). And the

reaction between these phases must be minimum. Because if the volume of the reaction products formed during infiltration is equal or greater than the initial volumes of the solid and the infiltrant liquid; penetration is stopped before completion [19].

Solubility: The effects of solubility generally helpful, when solid solution formation between components is minimum at low temperatures and when equilibrium conditions at the infiltration temperature produce minimum dissolution of the powder compact in the liquid infiltrant. If the powder dissolves in the liquid infiltrant in large amounts, the infiltration rate may be lowered and longer times requires for complete infiltration. Presaturation of the infiltrant with the compacted powder or alloying with a solubility - inhibiting element eliminates this problem [19].

Vacuum: When the system is subjected to a vacuum, capillary infiltration may be enhanced. Under vacuum, volatile impurities are easily removed from the melted infiltrant [19].

Pressure Gradient: By applying pressure, the infiltration becomes less dependant on capillary action and good wetting. The compacted powder with a less controlled pore structure can be infiltrated by applying pressure gradient with the aid of an external force acting on the liquid. And also systems in which the liquid forms high contact angles with the compacted powder can be infiltrated if the pressure is sufficient [19].

Many methods have been employed during the development of infiltration technique. Some of these techniques are reviewed below.

Capillary - Dip Infiltration: The solid body is partly immersed into a molten metal bath in a crucible as shown in Figure 2.4.a. Liquid is drawn in by capillary forces, removes the gas in the pores and rises [19].

Full - Dip Infiltration: The compacted powder is completely immersed in the molten metal as shown in Figure 2.4.b. Penetration occurs from all sides toward the inside. To avoid gas entrapment, immersion of the compacted powder must be slowly. Application of a vacuum helps degassing [19].

Contact Infiltration: The infiltrant is initially placed in contact with the solid, after melting, the liquid penetrates the solid. If the infiltrant is placed on top of the solid (as shown in Figure 2.4.c) surface tension may spread the liquid over all faces of the compacted powder before penetration. Gas displacement from the pores is aided by placing the infiltrant under the compacted powder or by applying vacuum [19].

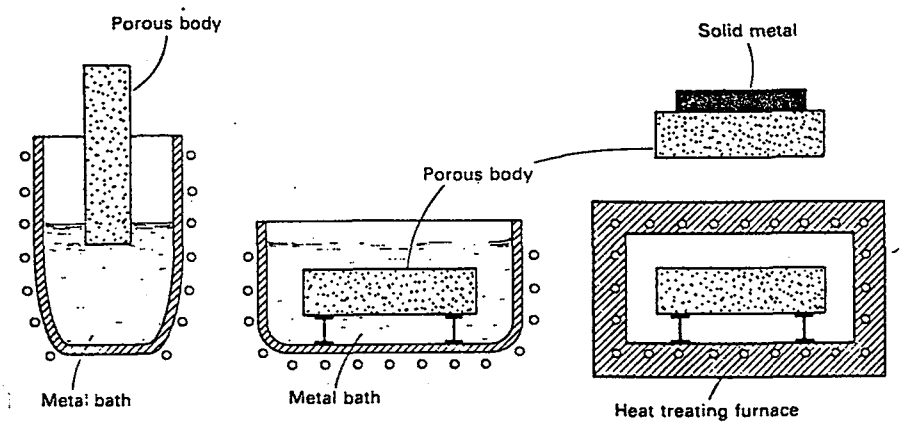

(a) (b) (c)

FIGURE: 2.4. Infiltration methods a) Capillary dip infiltration b) Full dip infiltration c) Contact infiltration

Vacuum Infiltration: Two methods can be employed to create a vacuum in metal infiltration. In the first method; by applying suction to the liquid phase, a pressure gradient is created and this allows atmospheric pressure on the molten metal infiltrant to be the driving force. For this method, a closed mold system which contains the molten infiltrant and the compacted powder is required. Then vacuum is applied to the end of compacted powder. The second method is simply placement of the entire infiltration system in a vacuum furnace. This method is useful for systems with strong outgassing components, but may cause difficulties in controlling the infiltration period and infiltrant temperatures [19].

2.5. General Properties of AlN and B_4C

AlN is covalently bonded material, it has wurtzite - like hexagonal lattice which is somewhat different from the ideal structure [20,21]. It has been regarded as a useful nitride ceramic because of its excellent properties. It has attracted much attention as a high-thermal conductivity ceramic substrate. The theoretical thermal conductivity of single crystalline AlN at room temperature is about 320 W / m.K. This value is 90% of BeO and 7 times that of Al_2O_3. However, this high value can be obtained only in pure single crystals [22,23,24]. Thermal conductivity of AlN depends on the amount of impurities especially oxygen and carbon. Oxygen atoms are dissolved in the lattice and reduce the thermal conductivity. The thermal conductivity of AlN decreases as the oxygen content increases and therefore the quantitative determination of the oxygen content in AlN is very important [21,22,25]. For polycrystalline AlN, thermal conductivity changes between 10 and 260 W / m.K depending on processing conditions and purity. Lower

values than theoretical thermal conductivities in crystalline solids are due to microstructural factors for example grain boundaries, porosity, lattice impurities or defects [23]. Only beryllia, copper and aluminum exceed AlN. But beryllia is an expensive and highly toxic material. Copper and aluminum are both soft and low melting point materials. Therefore, for areas where good mechanical properties at high temperatures with high thermal conductivity is required, AlN is the most appropriate material [26].

AlN sublimates at 2450°C without liquefying under non- oxidising conditions [27]. Since AlN is not dissolved or eroded by molten Al and unaffected by molten ferrous alloys, it has potential applications in various smelting operations [28]. It is stable in carbon monoxide up to 1800°C, in hydrogen to 1400°C, in vacuum to 1500°C and in nitrogen to 2700°C. As a non-oxide ceramic, this material may suffer attack from oxidizing environment. As a non-oxide ceramic, this material may suffer attack from oxidizing. The oxidation rate of AlN to Al_2O_3 occurs at a significant rate above about 1000°C and this reaction limits its continuos application at high temperatures in oxidizing atmosphere [29,30].

Other than its high thermal conductivity, AlN has a low thermal expansion coefficient ($\alpha = 4.3*10^{-6}$ /K at room temperature, near that of Si), it is an electrical insulator (electrical resistivity, r > 1013 Ω.cm at room temperature), a low dielectric constant (K'= 8.9 at 1 MHz at room temperature). These properties make AlN an important ceramic material in electronics industry. It is a candidate as a substrate for power circuits and as a packaging material for integrated circuits. Other application areas of AlN are; heat sinks, laser diode heat spreaders and fillers for polymer and glass

compounds [31,32]. Table 2.3. shows the properties of AlN in comparison with other ceramics [26,29].

TABLE: 2.3. Properties of AlN in comparison with other ceramics

	Density (gr/cm^3)	Thermal Conductivity (W/mK)	Thermal Expansion 10^{-6}/ °C	Elastic Modulus (GPa)	Hardness (Mohs)	Bending Strength (N/mm^2)
AlN	3.26	185	4.6	343	8	280-350
Al_2O_3	3.96	29	7	378	9	240-250
BeO	3	240	7.6	378	8-9	170-230
SiC	3.21	100	4.6	460	9	500
BN	2.25	14	12.2	82	2	
Si_3N_4	3.3	10-40	3.1		8-9	600-700

Since AlN is a covalent compound, limited atomic mobility prevents densification of pure AlN [32]. By hot pressing commercially available aluminum nitride powders at 2000°C, 97-99% of theoretical densities can be obtained. However, hot pressed aluminum nitride materials have anisotropic microstructure so their properties depend on direction. Since by hot pressing only simple shaped bodies can be produced, pressureless sintering processes have been developed. But pressureless sintering of aluminum nitride require sintering aids. Many compounds have been tested for promoting sintering especially oxides of elements from the second and third group of the periodic system were found to be effective. CaO, BaO, SrO form a liquid phase at high temperature and it is advantageous for densification of AlN. Onthe other hand, AlN is very sensitive to oxygen and oxygen dissolves in AlN powder to form a solid solution. It exists not only on the surface of the powder but also inner part of it. Moreover, oxygen may be in the form of Al_2O_3 during the preparation of AlN. While sintering at high temperatures, surface oxygen diffuses into the AlN grains and remains in the state of a solid solution or is converted to a compound having spinel type structure

defined by the formula $(AlN)_x(Al_2O_3)_y$ and resulting in impairing the excellent properties such as high thermal conductivity. When the concentration of oxygen exceeds 5%, it is difficult to remove all oxygen. In this case, carbon or a compound which can be converted into carbon by sintering is useful. It reduces and eliminates oxygen in the AlN starting material and also contributes to inhibit the formation of a compound having spinel type structure [33,34,35].

AlN can be manufactured commercially by either direct nitridation of aluminum powder at low temperatures or carbothermic reaction of alumina with carbon under nitriding conditions. Other effective method is a plasma process. In this process, Al metal is vaporized at temperatures close to 10000°K. The vaporized Al is then reacted with nitrogen gas, NH_3 or hydrogen gas and to form ultrafine AlN particles having a particle size $<0.1\mu$ and surface areas nearly $30m^2$ /gr [26,29,36].

The phase diagram of Al-AlN shown in Figure 2.5., indicates that there is no interaction between aluminum and aluminum nitride to the melting point of AlN at 2800°C. Thus a composite of aluminum and aluminum nitride would be thermodynamically stable and does not suffer destructive interfacial reactions and reaction products [7,26].

The wettability of several ceramics by liquid aluminum has been studied by Rhee [37] using sessile drop technique under vacuum conditions. According to his results, contact angle decreases linearly with increasing temperature in all ceramic/Al systems. He also found that Al/AlN system exhibits the least wetting.

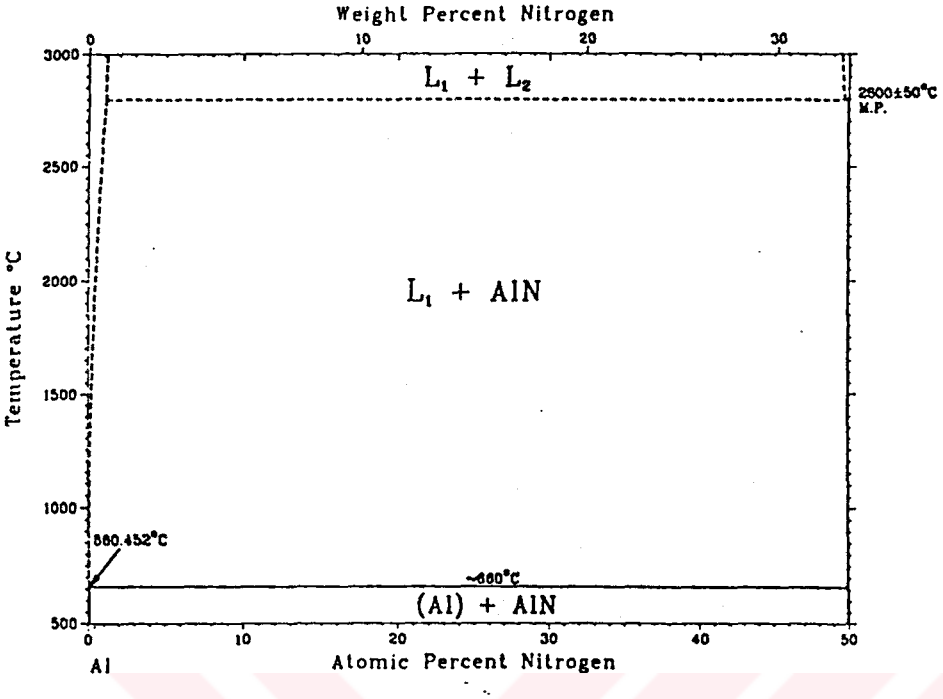

FIGURE: 2.5. Al/AlN phase diagram [7].

The other raw material used in this study is boron carbide (B_4C). It is a very hard material (9.5 in Mohs scale), low spesific gravity (2.52 gr/cm^3) covalently bonded ceramic material. It is an advantageous material for applications involving neutron absorption, wear and impact resistance. But B_4C is extremely sensitive to brittle fracture and producing fully dense B_4C is difficult. By using certain additives (for example graphite), sintered products with a high density (approximately 98.2% of the theoretical density) can be produced at temperatures above 2000°C. Hot pressing at about 2100°C is another technique to obtain high density products [38]. But since hot pressing is an expensive method , alternative methods are required. However, the studies on pressureless sintering of boron carbide have not been achieved yet. Mechanical properties can be improved with B_4C cermets. If the application is limited to low temperatures, a low melting point metal (for example aluminum) can be introduced to obtain lower

densification temperatures (< 1200°C) and to increase fracture toughness. And also if the metal has a low spesific gravity, then the cermet can have improved mechanical properties with low weight. Halverson et al. studied processing of B_4C-Al composites above 1000°C to promote wetting. As it was mentioned in Part 2.4., wetting is necessary to achieve strong interfacial bonding and to allow liquid rearrangement during sintering [38]. Figure 2.6. shows contact angle of aluminum on B_4C as a function of temperature and time

Aluminum starts to wetting B_4C above 1000°C under vacuum conditions. But under flowing argon, the contact angles are higher due to the oxidation of melted aluminum. In both cases, the contact angles decreases with increasing temperature and time. And also, by increasing the temperature, low contact angles are obtained in shorter times. However, since the vapor pressure of aluminum also increases with increasing temperature, to keep the vaporization of aluminum minimum, an upper processing temperature limit is necessary [38].

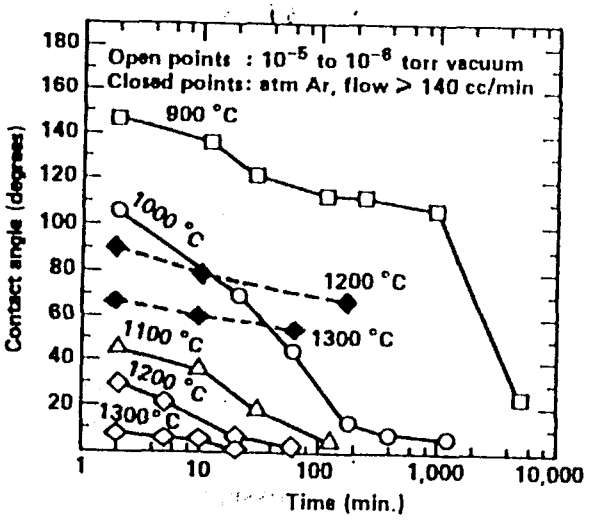

FIGURE: 2.6. Contact angle of aluminum on B_4C as a function of time and temperature [38].

Figure 2.7. shows, the relative amounts of phases which can occur during B_4C-Al cermet processing at temperatures between 800 and 1400°C. According to this figure, the amount of Al_4C_3 increase with increasing processing temperature. Al_4C_3 is undesirable, because of its hygroscopic nature and poor mechanical properties. And it is not stable at room temperature, therefore it is important to control the amount of this phase. An unidentified phase (called X), forms at all temperatures, B_4C and aluminum react to form this phase. Sarìkaya et al achieved to characterize the crystal structure and composition of phase X by transmission electron microscopy techniques. According to their results, the crystal structure of phase X is hexagonal close packed and the composition is Al_4BC. Under equilibrium between 800° and 900°C, the major reaction products are AlB_2 and Phase X. Under these conditions, phase X is stable, it decomposes after all of the free aluminum is depleted. Above 1100°C, the amount of phase X is less because aluminum is depleted through the formation of other stable phases. AlB_2 forms up to 1000°C,above this temperature it is not present in the microstructure. $AlB_{12}C_2$ is thermodynamically favored over AlB_2 between 900 and 1000°C. The amount of Al_4C_3 increases with a decrease of the phase X and $AlB_{12}C_2$ becomes a major phase above 1200°C. Al_4C_3 begins to crystallize in the shape of short whiskers. At temperatures above 1300°C, after all aluminum and phase X are completely depleted from the system, overall equilibrium occurs. Then Al_4C_3 decomposes and graphite, B_4C and $AlB_{24}C_4$ remain as stable phases [9,38].

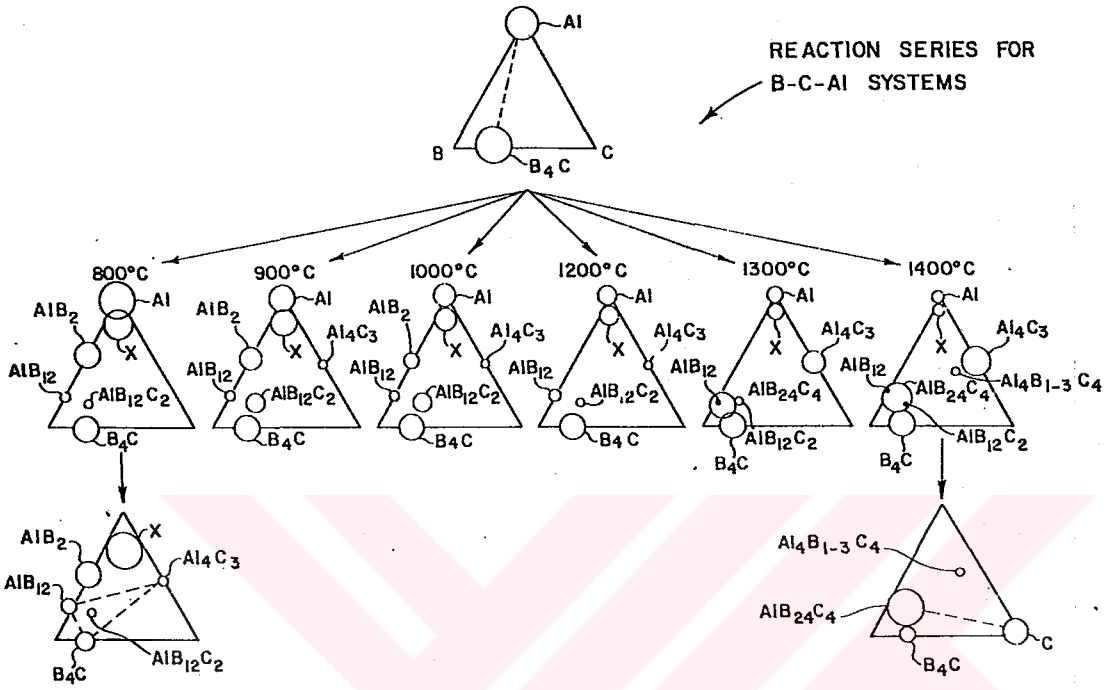

FIGURE: 2.7. Reaction series for B-C-Al systems [38].

CHAPTER 3. EXPERIMENTAL PROCEDURE

3.1. Preparation of Ceramic Preforms

AlN (Hermann Starck, Berlin, grade KT) and B_4C (ESK Co, average particle size is 5μ) powders were used as raw materials. Manufacturer's spesification for chemical composition and average particle size of AlN is shown in Table 3.1.

TABLE: 3.1. Characteristics of AlN powder

CHEMICAL COMPOSITION (%)	
N	33
C	0.05
O	0.7
Fe	0.010
Other metallic impurities	< 0.05
Medium particle size (μ)	13.6

In Figure 3.1., the processing flow diagram for AlN-B_4C / Al composites is shown. Since AlN has low reactivity with isopropanol alcohol, batches containing different amount of B_4C (1,2,4 and 10 wt%) were mixed in alcohol. AlN and B_4C powders were mixed by magnetic stirrer, then binder (carbowax 8000, polyethylene glycol, 4wt%) was added during ultrasonic agitation. The suspension became uniformly dark after ultrasonic mixing due to the fine B_4C powder. The mixed suspension

then heated to about 60°C to evaporate alcohol, the dried mixture was sieved through an ASTM No: 20 grit sieve.

About 5 grams of mixture uniaxially pressed under about 1800kg (4000lb) in a steel die to form cup shaped samples. To eliminate density inhomogenities and for handling purposes, the samples were subsequently cold isostatic pressed (National Forge Company) at about 172 MPa (≈ 25000 psi) Simultaneously, some spare samples also pressed for each composition for characterization of the sintered preform microstructure by mercury porosimetry.

Binder was partially burned out before firing. Prepared samples were heated to 200°C and held at this temperature for 1 hour. According to weight changes, about 3.7 wt% of added binder was decomposed during this process. The strength of the residual binder makes the measuring and holding processes possible. Most of the residual binder was decomposed during the following sintering process under nitrogen atmosphere.

The samples were loaded into a graphite crucible and put on AlN powder which is used as a bedding powder. Sintering experiments were carried out in an induction heating system shown in Figure 3.2. Regular grade nitrogen was pre-purified by passing through drierite and copper turnings at about 350°C at a rate of approximately 85 liter / h. The furnace which is shown in Figure 3.3. was connected by a water cooled copper tube coil to a 15KW Induction Power Track System (VIP 15-96 Power Track Induction Furnace, Inductotherm Corporation, Rancocas N.J.). The crucible with specimens was set on graphite felt on top of the susceptor. Temperatures were measured by Pyro Micro-Optical pyrometer through the silica glass on top of the furnace, sighting through the holes into

the crucible. Mo plates attached to the system and they were used for heat shielding in front of the silica glass. Water cooling copper were soldered on the top of the chamber and an active water cooling jacket was around the outside of the chamber. A mechanical pump attached to the furnace was used to eliminate the residual oxygen and water vapor before the chamber was back filled with purified nitrogen. The furnace was evacuated with a mechanical pump after the crucible was loaded into the furnace. Nitrogen gas was purged through the system for about an hour before starting to heat. Several sintering temperatures were tried (1400 to 1600°C), heating rate was 12°C /min and the holding time at these temperatures was 1 hour. 1 atmosphere nitrogen pressure was continuously maintained within the chamber. At the end of the soaking period, the system was cooled down to room temperature.

3.2. Molten Metal Infiltration

The same induction furnace was used for the wetting infiltration of liquid aluminum into the preform. The infiltration was accomplished by placing a known amount of aluminum (99.99 % pure) on top of the sample. The shape of the preform was shaped like a small reservoir to hold the molten aluminum in place at high temperatures. Amount of aluminum used varied from 2.5 to 3.5 grams which is more than required to fill the open porosities. Similar to sintering experiments, sintered ceramic preforms with aluminum metal were placed inside the crucible on AlN powder.

Several infiltration atmospheres were investigated. Tha chamber was evacuated with a mechanical pump. 50 torr and 400 torr Ar chamber pressures were provided with a second mechanical pump attached to the system. Ar gas

purified by passing through drierite and copper turnings at about 350°C and titanium furnace about 780°C. The furnace was heated to 900°C under vacuum to avoid Al_2O_3 formation on molten aluminum surface, then Ar gas was entered and heating continued to about 1250°C. The heating rate was 12°C/min and infiltration time was 20 minutes. The process can be observed from the glass window on the top of the furnace. After each holding time at the infiltration temperature, the furnace turned off and the system was left to cool down to room temperature. Ar gas was continued to give to furnace to avoid the oxidation of aluminum until the temperature decreases to below 600°C.

3.3. Characterization of Powders and Preforms

The chemical composition and particle size of AlN was given by the manufacturer and is given in Table 3.1. The spesific surface areas of AlN, B_4C and sintered products were measured by 3- point BET method with a Quantachrome Autosorb 1 instrument.

Mercury porosimetry was used to characterize the microstructures of sintered preforms with a Micromeritics Autosorb II 9220 instrument. It is a recognized method for determination of pore size distribution. Mercury porosimetry is conducted by first preparing a sample of a size dependant on the material porosity and with pore volume measurable by the equipment. The sample is placed in a holder called penetrometer, evacuated and then immersed in mercury at a low pressure. Increasing pressures are applied on the mercury and the corresponding volumes of intruded mercury determined [39].

Before and after sintering, each sample was carefully weighed to determine weight change. Sintered products were examined by JEOL -JSM T-330 scanning electron microscopy.

3.4. Characterization of Infiltrated Samples

The infiltrated samples were cut through the middle with a diamond saw. Half of the samples were mounted and polished to 1200 grit SiC paper then polished on a cloth with Al_2O_3 dispersed distilled water. The microstructures were examined by optical microscope and SEM. Since there is a high contrast between light reflecting aluminum and grey aluminum nitride, no etching was used. Infiltrated samples also were analyzed with X ray diffraction (Rigaku-RINT XRD, CuK_α radiation). Hardness of the composites were measured with a Macro Vickers Hardness equipment with 50 kg load.

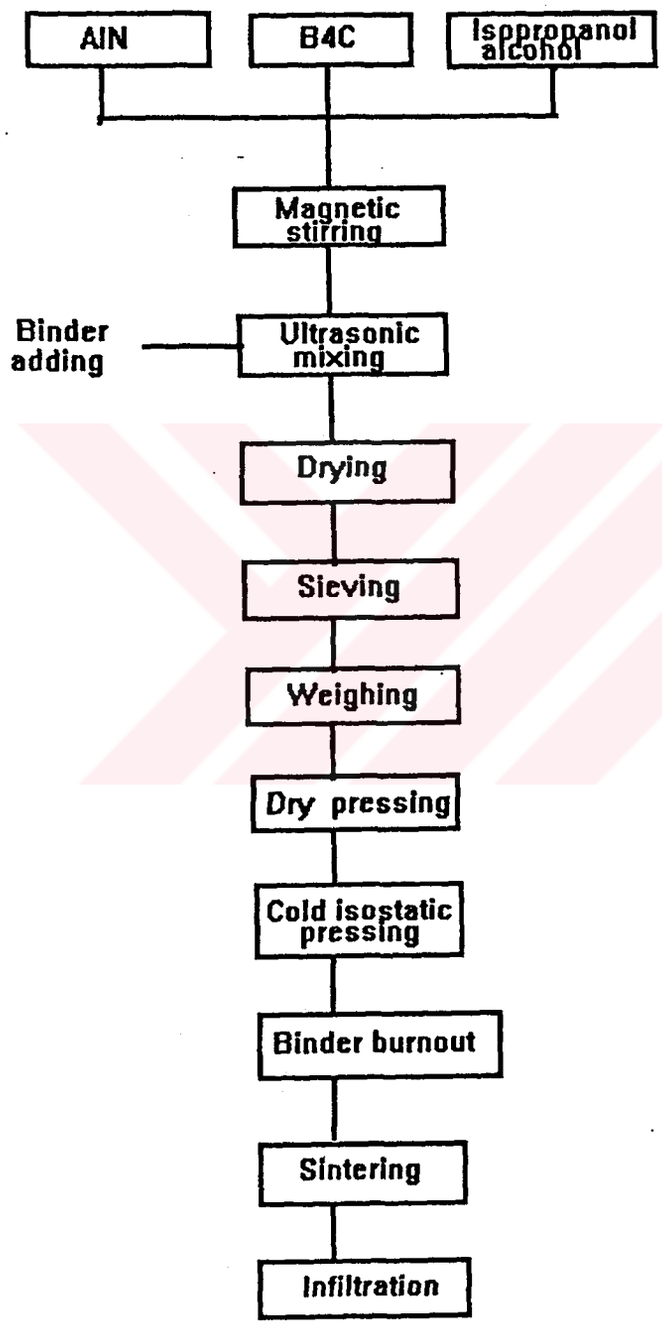

FIGURE: 3.1. Processing flow diagram

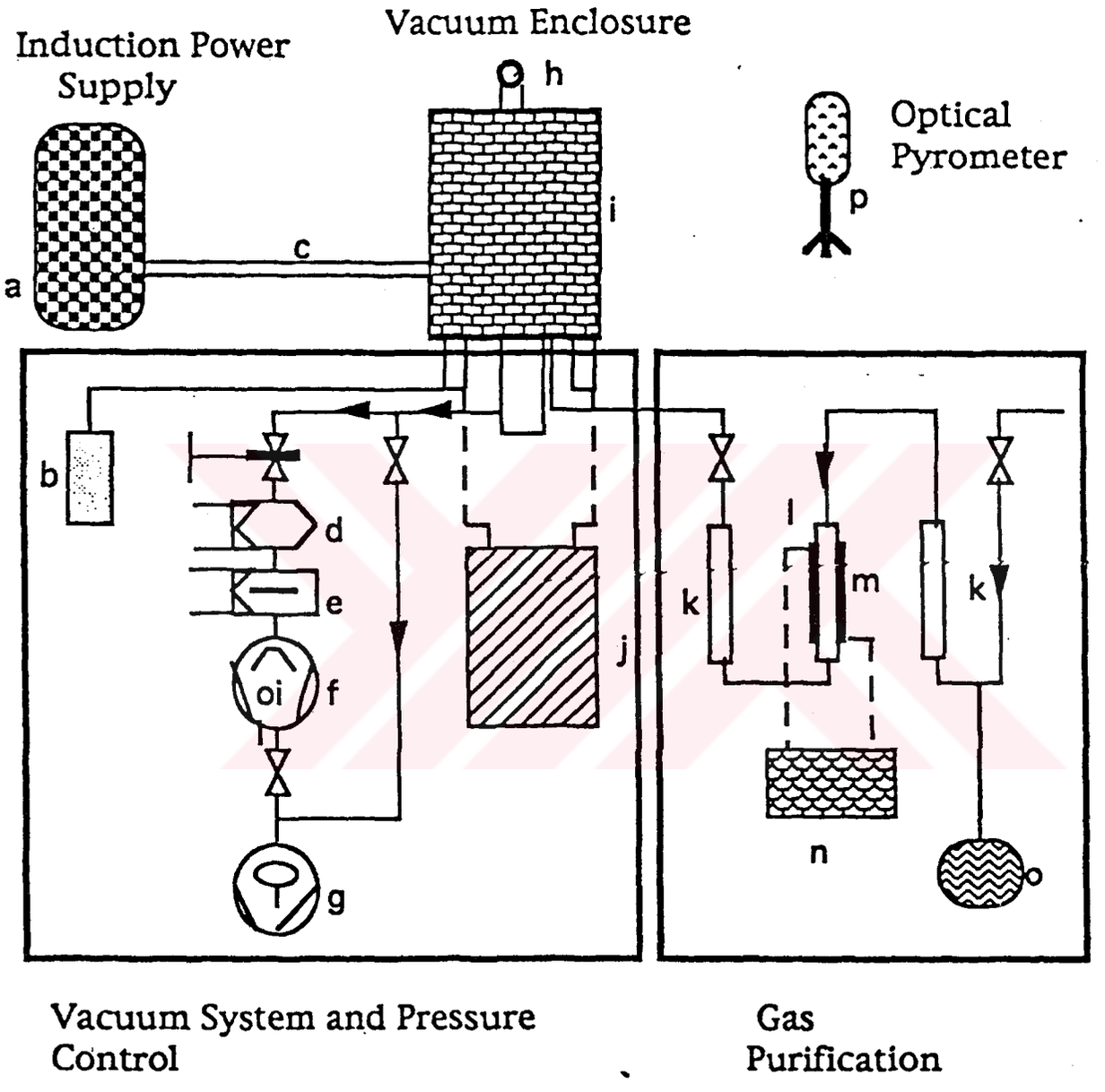

FIGURE: 3.2. Schematic diagram of experimental set-up (a) Induction power supply (b) electronic manometer (c) copper tube (d) baffle (e) diffusion pump (f) mechanical pump (g) mirror (h) furnace (i) vacuum gauges control assembly (j) drierite (k) copper turnings (l) heating tape (m) variable AC transformer (n) timer (o) optical pyrometer

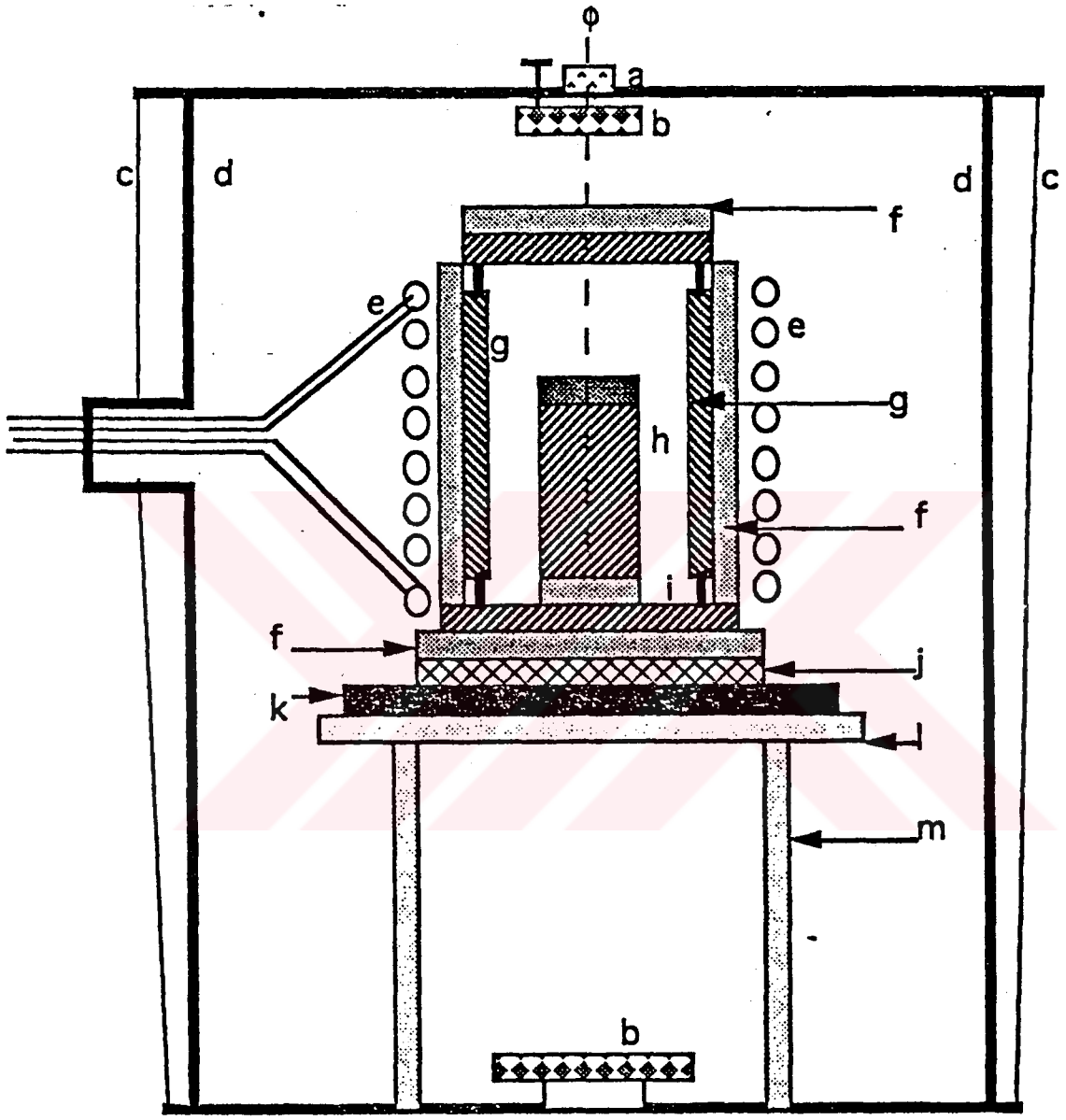

FIGURE: 3.3. The schematic picture of the furnace (a) silica sight glass (b) Mo radiation shield (c) water jacket (d) bronze chamber case (e) copper tube and induction coil (f) graphite felt (g) graphite susceptor (h) graphite crucible (i) graphite step (j) honeycomb cordierite insulator (k) SiC plate (l) steel plate (m) steel rods

CHAPTER 4. RESULTS AND DISCUSSION

The cold isostatic pressed ceramic preforms were weighed before and after sintering to determine weight change. Results have indicated that the preforms which have higher B_4C content weight gained. Although the samples containing 10 wt% B_4C weight gained at all sintering temperatures, the samples containing 1 wt% B_4C weight lost. The percentage of weight change has increased with increasing sintering temperature.

Nitrides are generally contain some oxygen. According to manufacturer's spesification the AlN we used in this study contains 0.7% oxygen. For AlN, the oxygen is usually in the form of Al_2O_3 on powder surfaces. Since Al_2O_3 prevents infiltration, the amount of oxide must be reduced. Numerous studies have been reported in the literature about the contact angle of aluminum on aluminum oxide. The contact angle exceeds 90° at temperatures below 950°C to 1000°C. It was reported that, a thin film of oxide on AlN surface acts as a non-wetting barrier.

Toy at al [7]. had mixed AlN powder with a known amount of carbon and fired under nitrogen at 1700°C for to convert aluminum oxide to aluminum nitride according to reaction 4.1.

$$Al_2O_3 + 3C + N_2 \longrightarrow 2AlN + 3CO \qquad (4.1.)$$

In our experiments B_4C was used and it is assumed that aluminum oxide reacts with B_4C and yields to AlN and BN as

shown in reaction 4.2.

$$Al_2O_3 + 3B_4C + 7N_2 \longrightarrow 2AlN + 12BN + 3CO \qquad (4.2.)$$

The standart free energy of this recation indicates that it is possible to convert Al_2O_3 to AlN and BN. The free energy change has been calculated as - 839 kJ/mole at 1900°K (1627°C). According to reaction 4.2. for a complete reaction the weight gain is 41.8 %. Therefore the weight gain while sintering indicates the conversion. And since Al_2O_3 is detrimental to infiltration the higher the weight gain must result in better infiltration. This result is exactly in consistent with our observations as shown in Table 4.1.

TABLE: 4.1. The relationship between weight change and infiltration

Mixture	Temperature (°C)	Observed weight change (%)	Infiltration
AlN+10%B_4C	1400 1500 1600	weight gain at all temperatures	Infiltrated
AlN+4%B_4C	1400 1500 1600	weight loss weight gain weight gain	Partially inf. Infiltrated Infiltrated
AlN+2%B_4C	1400 1500 1600	weight loss weight loss weight gain	No inf. No inf. Infiltrated
AlN+1%B_4C	1400 1500 1600	weight loss at all temperatures	No infiltration

If it is assumed that, the oxygen in the AlN powder (0.7%) is all in the form of Al_2O_3, it is calculated from stoichiometry that the amount of Al_2O_3 initially present was 1.48% . The theoretical amount of B_4C required to fully react with the Al_2O_3 is about 1.62 times higher than the amount of Al_2O_3. The ratio of B_4C/Al_2O_3 for each mixture was calculated in terms of reaction 4.2. and results are shown in Table 4.2.

TABLE: 4.2. The theoretical B_4C/Al_2O_3 weight ratio

Samples	B_4C/Al_2O_3
AlN + 1%B_4C	0.684
AlN + 2%B_4C	1.38
AlN + 4%B_4C	2.81
AlN + 10%B_4C	7.52

The results show that, for samples containing 4 and 10 % B_4C, aluminum oxide can be consumed because their B_4C/Al_2O_3 ratio is higher than the theoretical amount, 1.62. Therefore, it is thought that, weight loss observed in 1 and 2% B_4C samples is due to insufficient conversion of Al_2O_3 i.e. Al_2O_3 could not be reduced. It is necessary to mention here that, the samples weight lost during sintering did not infiltrate possibly due to the oxide layer on the powder surface.

The infiltration was observed through the quartz window on top of the furnace. at about 900°C, the surface of melted aluminum became dark which is due to the oxidation of aluminum. In all infiltration experiments, the

heating was done under vacuum to 900°C to avoid this oxidation. But it is well known that aluminum is easily oxidized. The oxide film formed on the surface of aluminum prevents the decreasing of contact angle.

$$4Al + 3O_2 \longrightarrow 2Al_2O_3 \qquad (4.3.)$$

Fujii et al. [40], calculated the oxygen partial pressure in equilibrium (P_{02}), assuming the activity of aluminum and aluminum oxide are one due to the fact that the solubility of oxygen in aluminum is very low. According to their results the oxygen partial pressure is about 10^{-27} Pa at 1373°K which is actually cannot be obtained.

Figure 4.1. shows the contact angle between AlN/Al compared with the contact angle between BN/Al at 1373°K. It can be seen that, BN/Al system have lower contact angle. Therefore, the production of BN in our system may cause better wetting and as a result of this better infiltration.

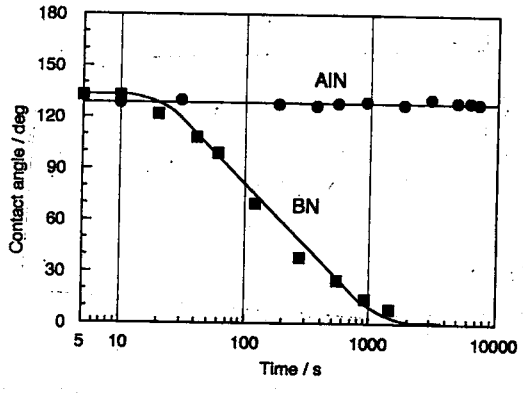

FIGURE: 4.1. Contact angle curves of AlN/Al and BN/Al at 1373°K [40].

4.1. X- Ray Diffraction Studies

The infiltrated samples were cut through the middle and sections were polished. In order to analyzethe aluminum content in the samples, X-ray diffraction analysis was used. In Figure 4.2., the XRD patterns of fully and partially infiltrated samples were shown.

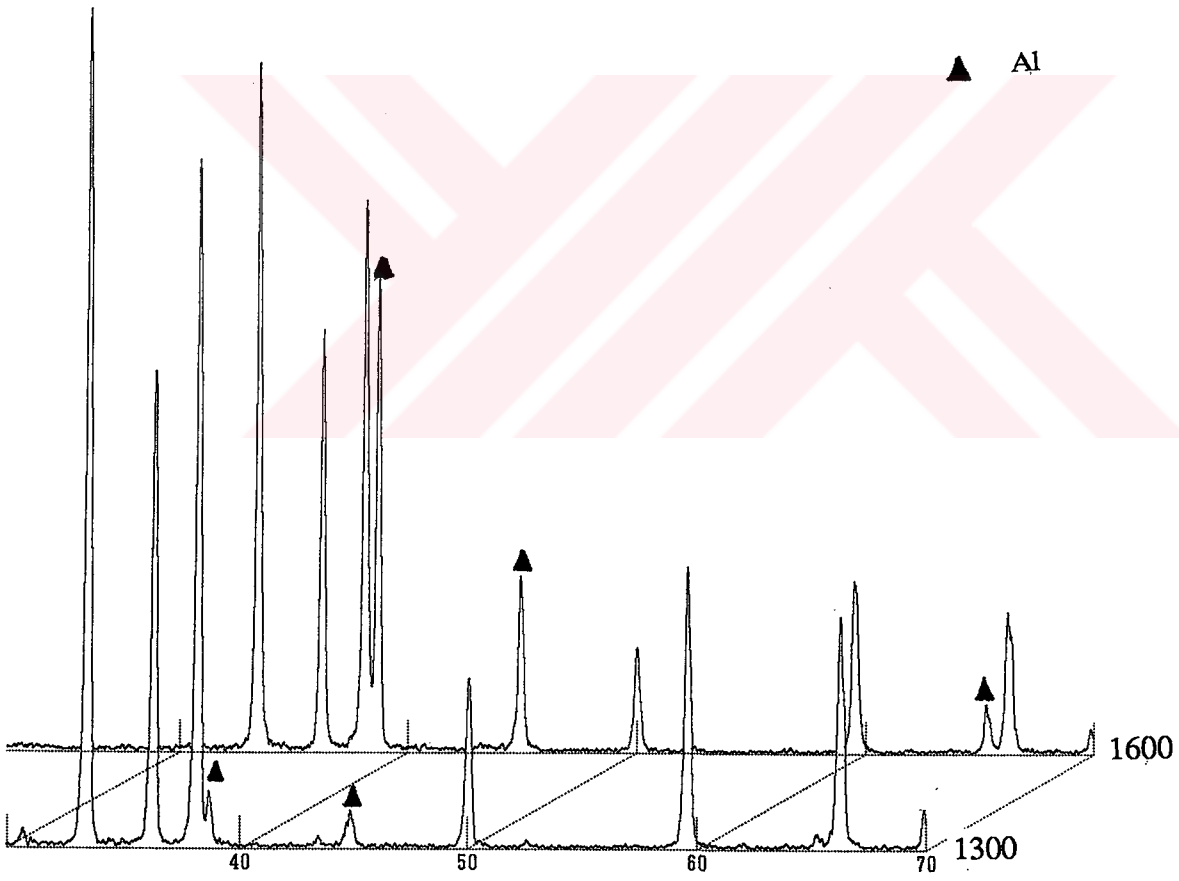

FIGURE: 4.2. The XRD pattern of partially and fully infiltrated AlN + 4% B_4C samples

Both of the samples have 4% B_4C and infiltrated under the same conditions, however the sample which has been sintered at 1600°C is fully infiltrated. We observed a weight loss at 1300°C but weight gain at 1600°C. In XRD patterns fully infiltration reveals itself much intense aluminum peaks as shown in Figure 4.2.

4.2. Mercury Porosimetry and Surface Area Studies

As it was mentioned in Chapter 2, for a succesful infiltration, the compacted powder should have interconnected pores and the size range of the powders should allow capillary force. Pore diameter in the preform is believed to control the flow rate of aluminum. Therefore, mercury pore intrusion was used to characterize the preform microstructure.

A small piece of preform (≈ 0.8 gr) was weighed and placed in a glass penetrometer, evacuated and then immersed in mercury at a low pressure. Increasing pressures are applied on the mercury and the corresponding volumes of intruded mercury determined. The relationship between pore diameter and pressure is given by the Washburn equation.

$$d = \frac{-4\ \gamma\ \cos\theta}{P} \qquad (4.4.)$$

where:

d= The diameter of a pore (μ)

γ= Surface tension of mercury (0.485 N/M)

P= The pressure required to force mercury into a pore

θ= The contact angle between mercury and solid (140°)

Since the surface tension and contact angle are constant, the pore diameter is inversely proportional with the pressure [39]. The equipment used in this study was capable of pressures to 60.000 psi. The conventional method for pore size distribution is to plot pressure vs cumulative volume intruded with mercury. But a plot of pore diameter vs cumulative pore volume is advantageous because any fraction of pore volume in a pore size range can be quickly estimated. The equipment is capable of estimate the average pore diameter, pore area and plot cumulative volume vs diameter and differential intrusion vs diameter.

The penetration of a fluid into a porous solid has been modeled by Washburn [39,41].

$$x^2 = \frac{\gamma_{lv} \cdot D \cdot t \cdot \cos\theta}{4\eta} \qquad (4.5.)$$

where:

x= Infiltration depth

t= Infiltration time

η= Viscosity

θ= Wetting angle

γ= Surface tension

D= Diameter

According to this equation, the infiltration distance is directly proportional to the square root of time, pore radius, surface tension and inversely proportional to the square root of viscosity. Therefore, mercury porosimetry was used to characterize the preform microstructure.

The results for 1,4 and 10 wt % B_4C sintered at 1400°C and 1600°C were shown in Figures 4.3 - 4.8. According to results, the pore diameter increases with increasing

sintering temperature due to grain growth at high temperatures. And pore diameter decreases with increasing B_4C amount. Since the average particle size of B_4C (5μ) is smaller than the size of AlN (13.6μ), the B_4C particles are locating between AlN particles and this results in smaller pore diameters in the preforms.

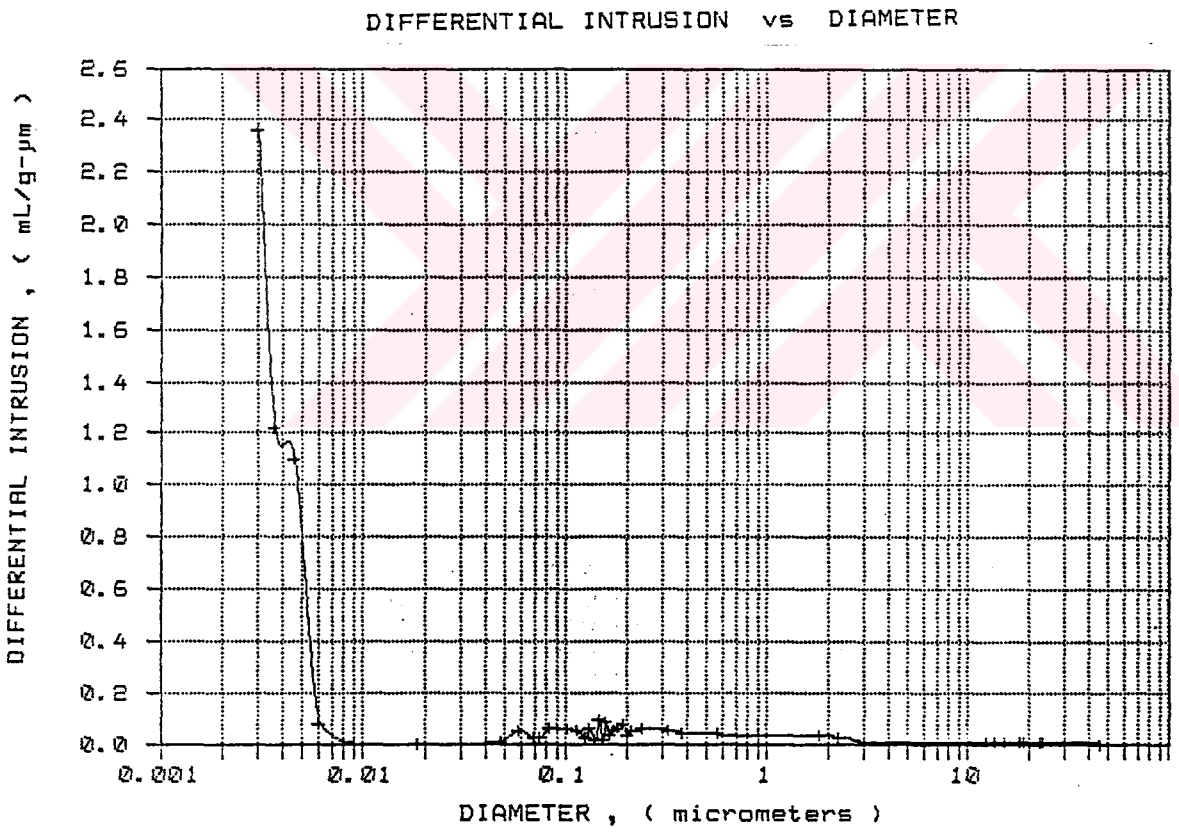

FIGURE: 4.3. Pore size distribution of AlN + 1% B_4C sintered at 1400°C

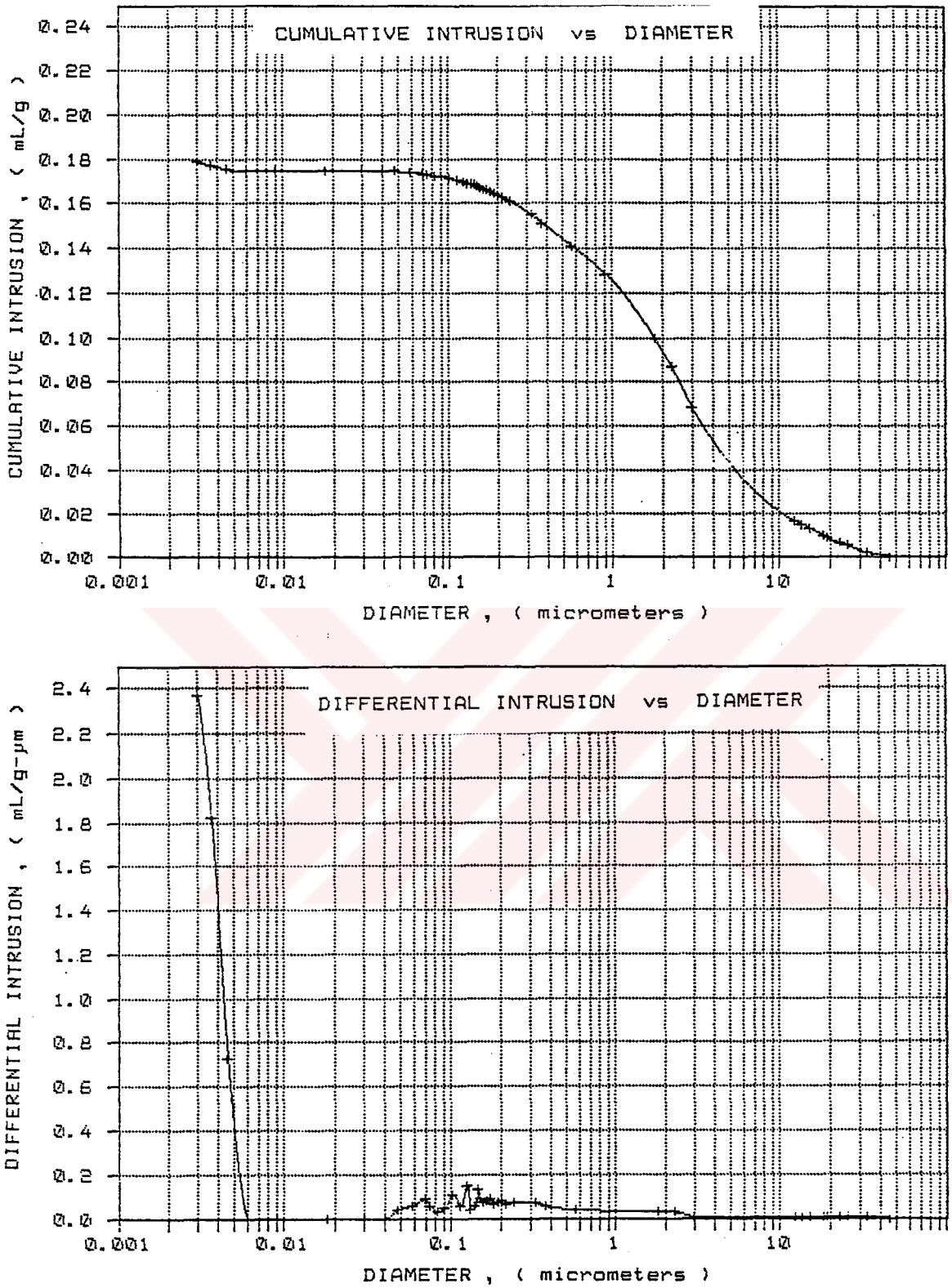

FIGURE: 4.4. Pore size distribution of AlN + 4 %B_4C sintered at 1400°C

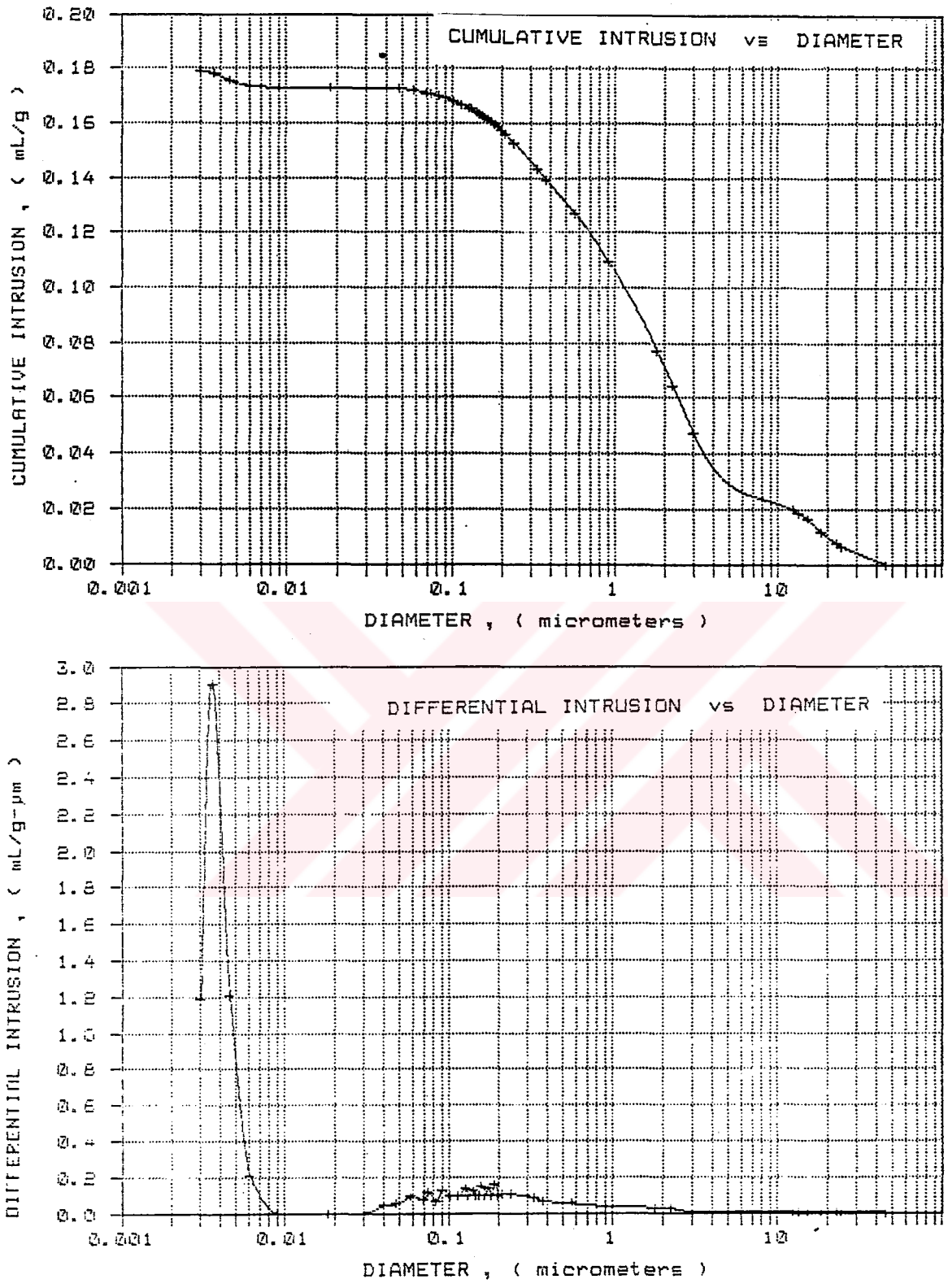

FIGURE: 4.5. Pore size distribution of AlN + 10B_4C sintered at 1400°C

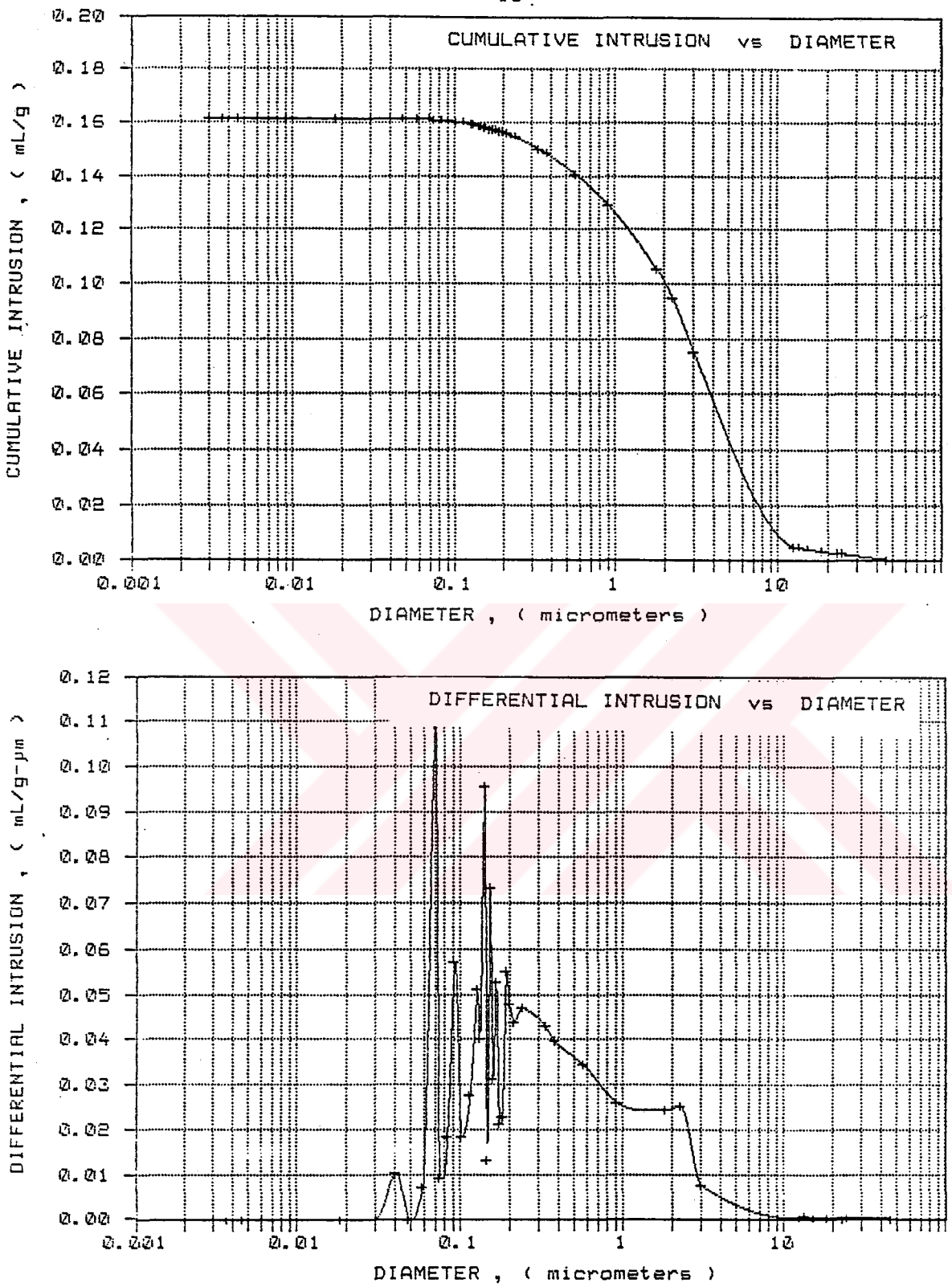

FIGURE: 4.6. Pore size distribution of AlN + 1 %B_4C sintered at 1600°C

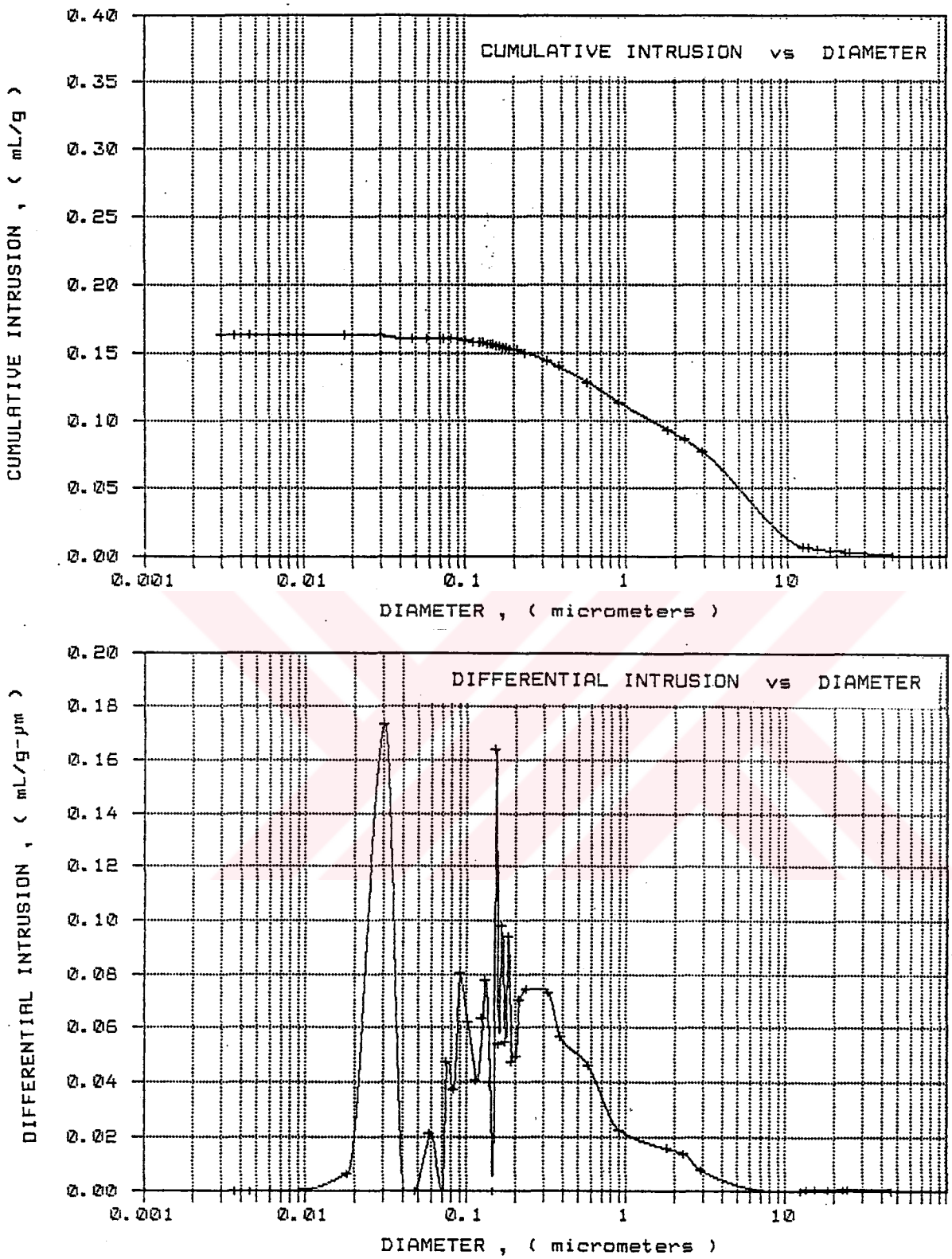

FIGURE: 4.7. Pore size distribution of AlN + 4 $\%B_4C$ sintered at 1600°C

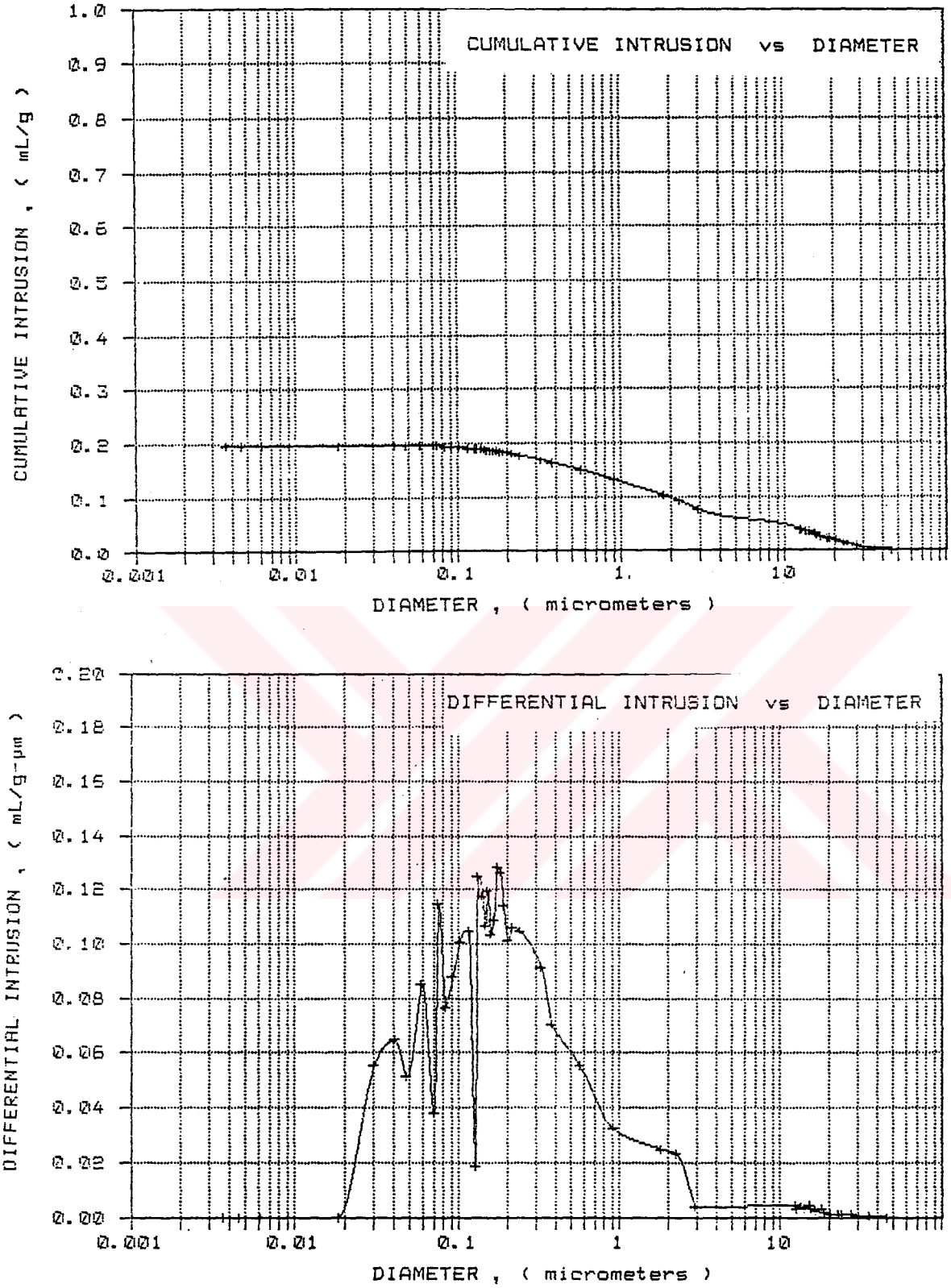

FIGURE: 4.8. Pore size distribution of AlN + 10 %B_4C sintered at 1600°C

The average pore diameters of the sintered products were measured and in Figure 4.9., the relationship between pore diameter and %B_4C content is shown.

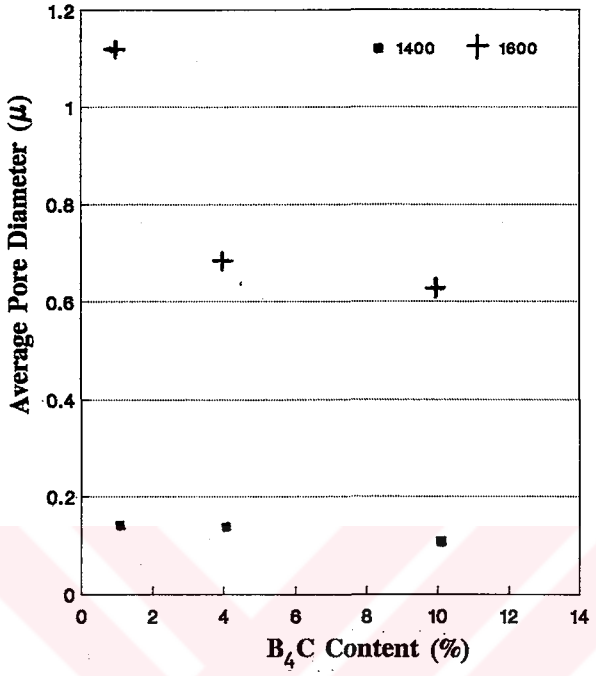

FIGURE: 4.9. Pore diameter - % B_4C relationship

Although the samples sintered at 1400°C have nearly the same average pore diameters regardless of the B_4C content, there is a gradual decrease in the samples sintered at 1600°C. It was mentioned previously that the infiltration distance is directly proportional to the pore radius, however it was observed that the samples containing larger amounts of B_4C (smaller pore size) fully infiltrated. This indicates that, pore size effects the rate of infiltration but it is not the only requirement.

Spesific surface areas of the sintered products were measured with 3 point BET method in order to investigate the effect of sintering temperature on particle size. The surface areas of raw materials, AlN and B_4C were measured as 0.7383 and 15.47 m^2/gr respectively which are in

consistent with the particle sizes. The results are given in Table 4.3.

TABLE: 4.3. Spesific surface areas of the sintered products as a function of temperature and B_4C content

Samples			
	1400	1500	1600
AlN + 1% B_4C	0.7809	0.7028	0.6042
4AlN + 2% B_4C	0.8055	0.7834	0.6156
AlN + 4% B_4C	0.9519	0.9068	0.7913
AlN + 10% B_4C	1.472	1.454	1.383

As it can be seen from the table that, the surface area is slightly decreasing with increasing sintering temperature and decreasing B_4C content. Since B_4C has smaller particle size, it is expectable an increase in the surface area while the content of B_4C increasing.

4.3. SEM Studies

JEOL - JSM (T330) scanning electron microscopy was used to observe sintered and infiltrated samples. The SEM studies showed that the sintering started newly at 1600°C. As we already mentioned that, pressureless sintering both AlN and B_4C requires sintering aids or they are sintered with the help of some other methods like hot pressing. Therefore, sintering temperatures of 1600°C provides somewhat continuous microstructure which is desirable for infiltration. Figure 4.10 shows this difference between 10 % B_4C sintered at 1400 and 1600°C. Figure 4.11 shows, 1% B_4C and 4% B_4C both sintered at 1400°C.

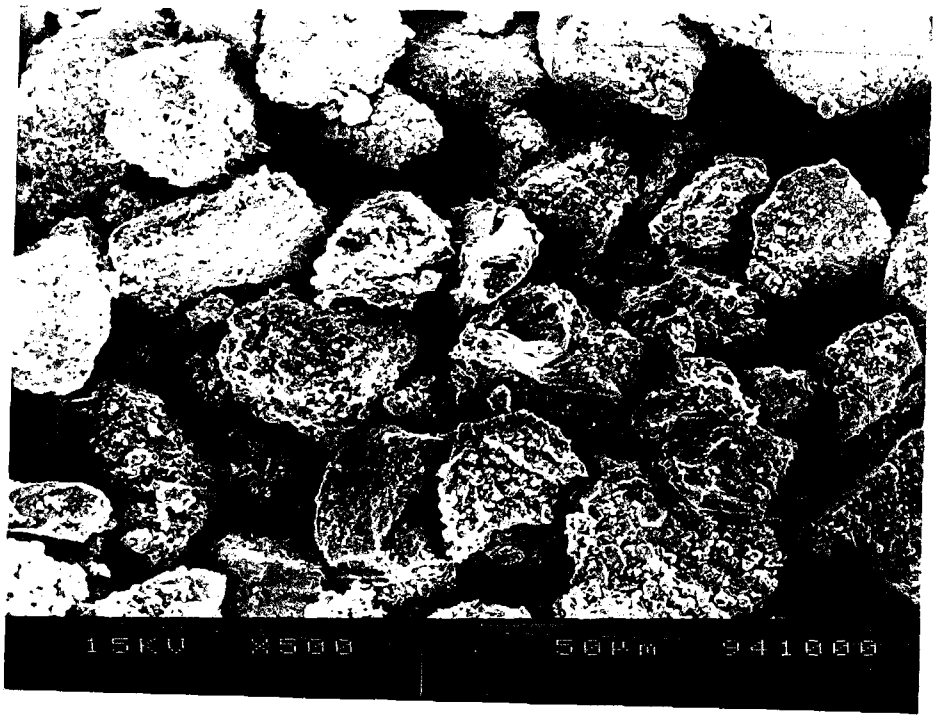

a

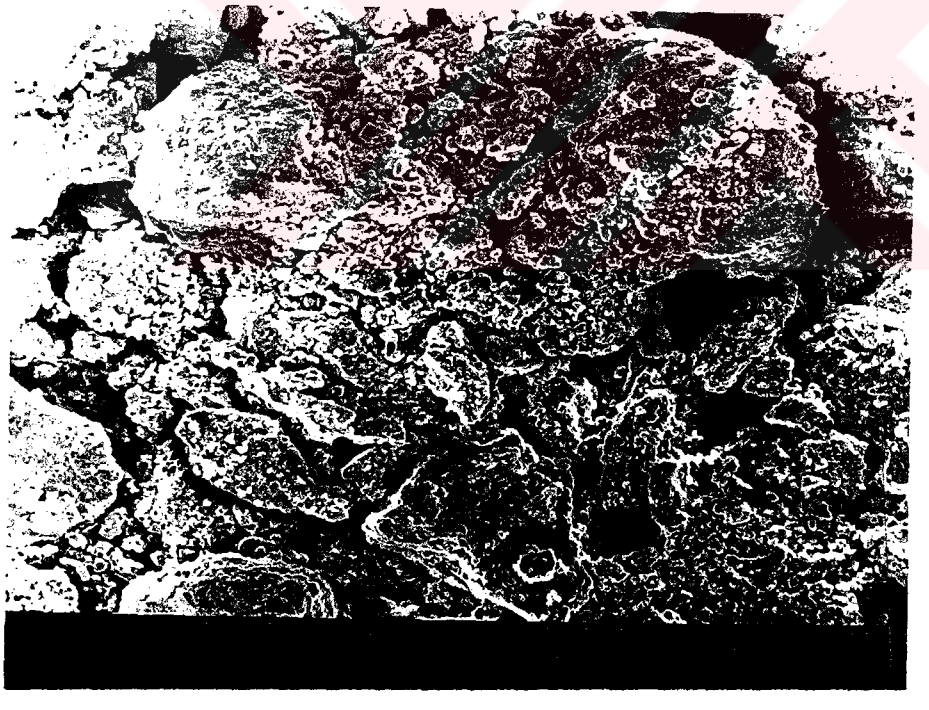

b

FIGURE: 4.10. AlN + 10% B_4C a) sintered at 1400°C
b) sintered at 1600°C

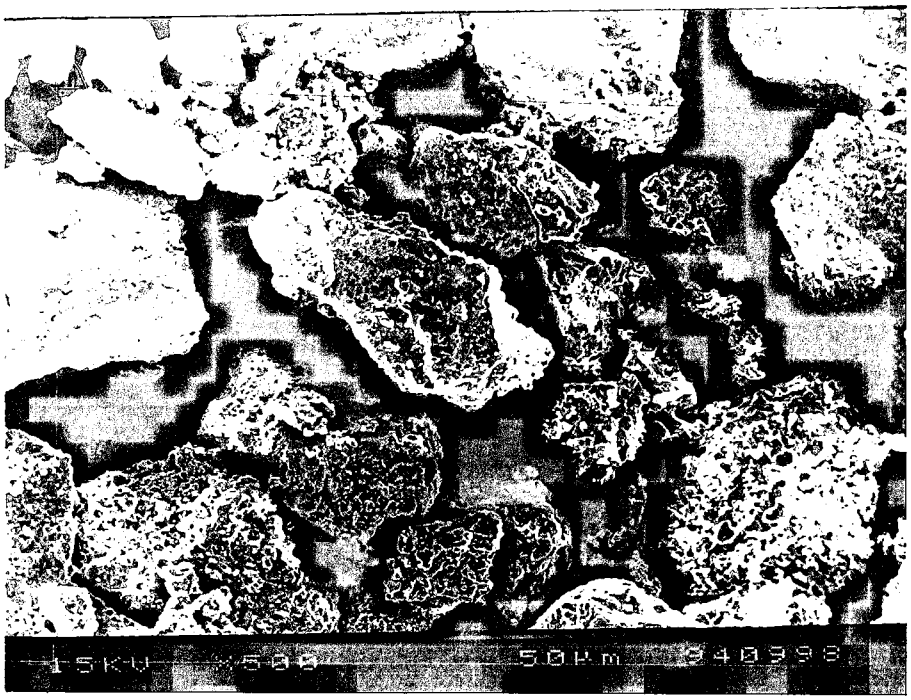

a

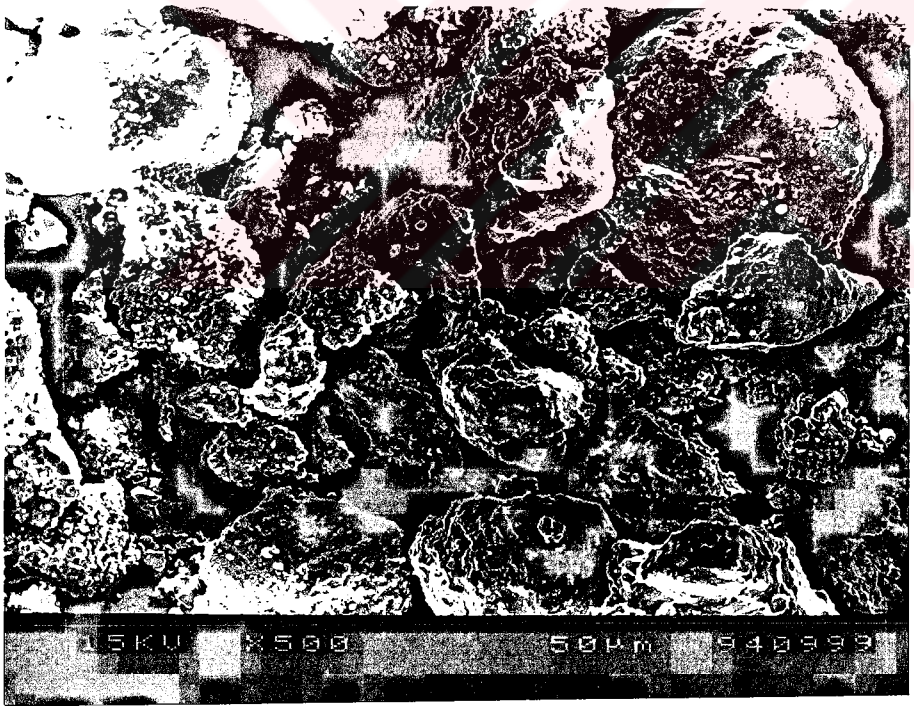

b

FIGURE: 4.11. a) AlN + 1% B_4C b) AlN + 4% B_4C both sintered at 1400°C

The sections of the infiltrated samples are shown in Figure 4.12. Both of the samples have 4% B_4C and infiltrated under the same conditions.

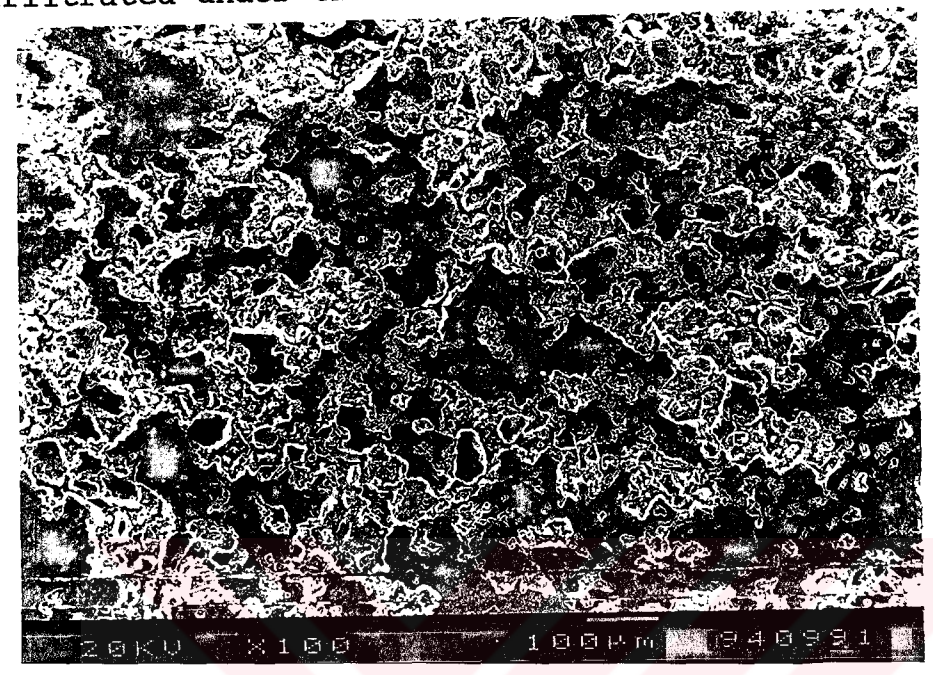

a

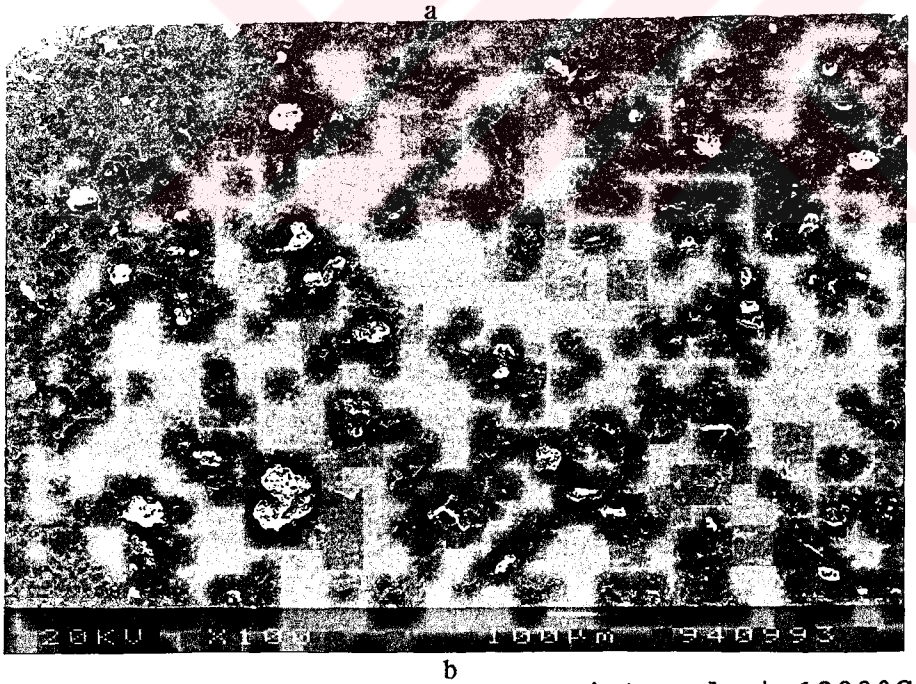

b

FIGURE: 4.12. AlN + 4% B4C a) sintered at 1300°C
b) sintered at 1600°C
Infiltration conditions: 1250°C, under 50torr Ar, 20 minutes

4.4. Optical Microscopy Studies

Mounted and polished samples were examined with optical microscope. Since there is a high contrast between aluminum and grey AlN, no etching was used.The microstructures are shown in Figures 4.13 - 4.15.

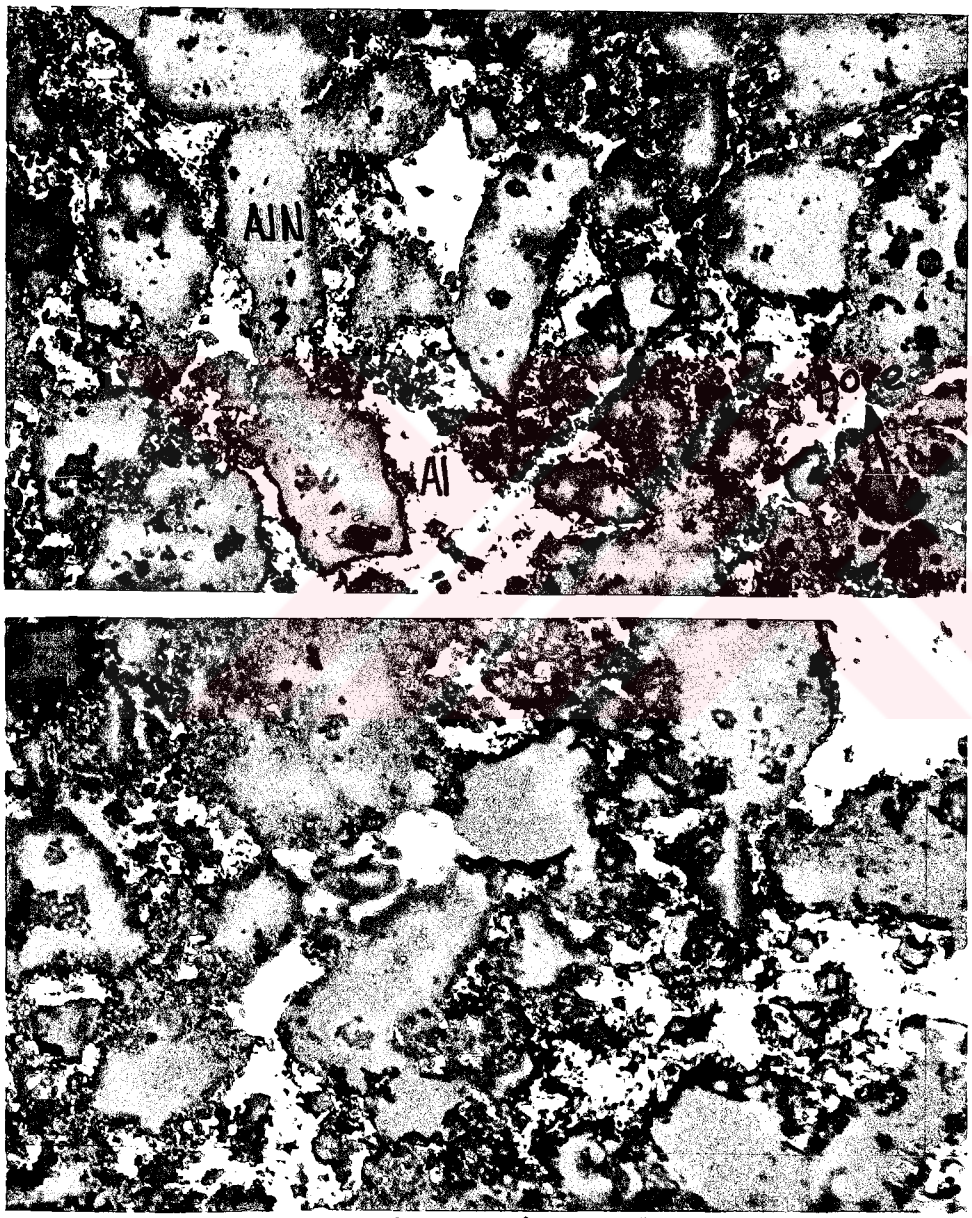

FIGURE: 4.13. AlN + 4% B_4C sintered at 1600°C
Infiltration conditions: 1250°C, 50torr Ar, 20 min

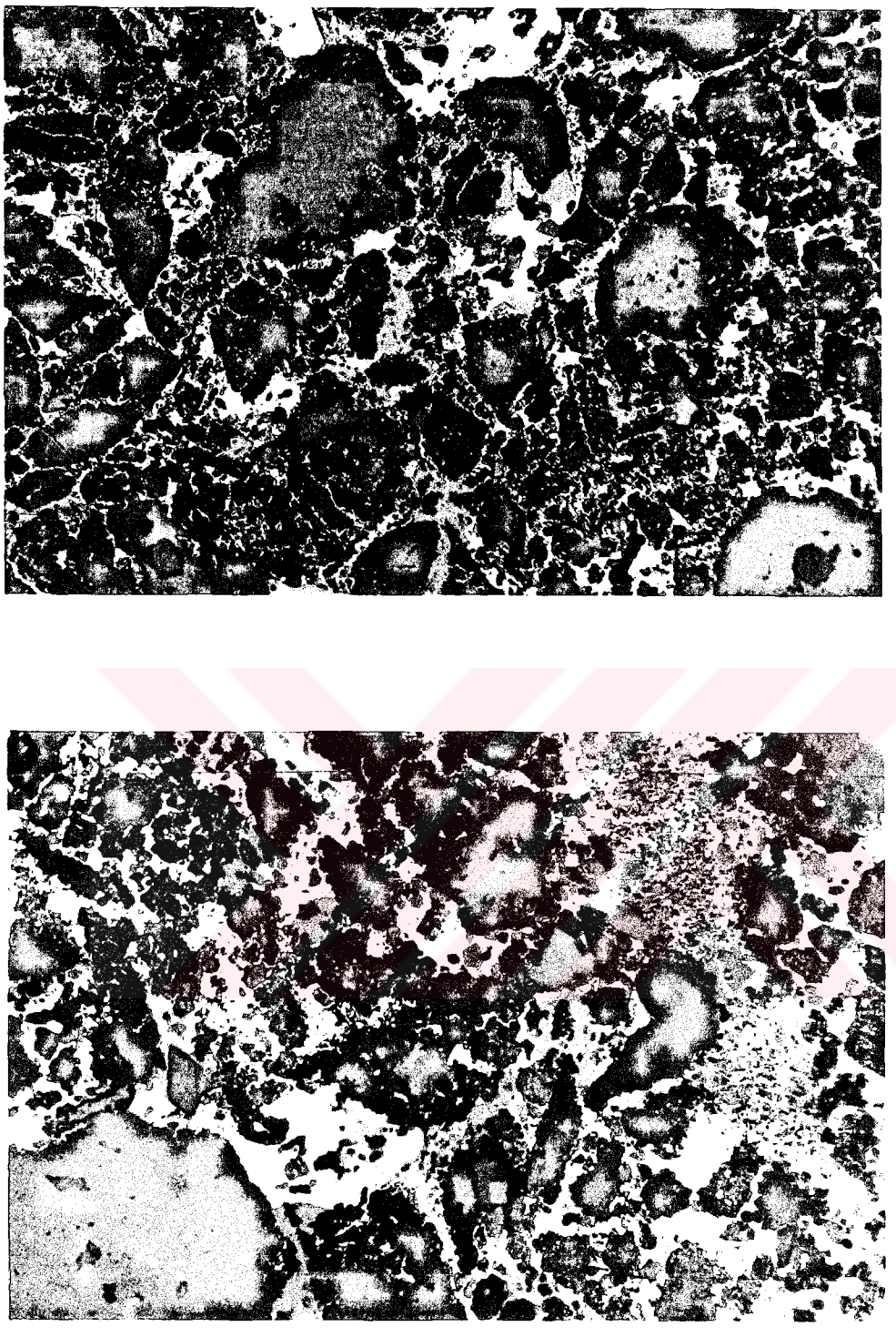

FIGURE: 4.14. AlN + 10% B4C sintered at 1600°C
Infiltration conditions: 1250°C, vacuum : Ar, 20 min

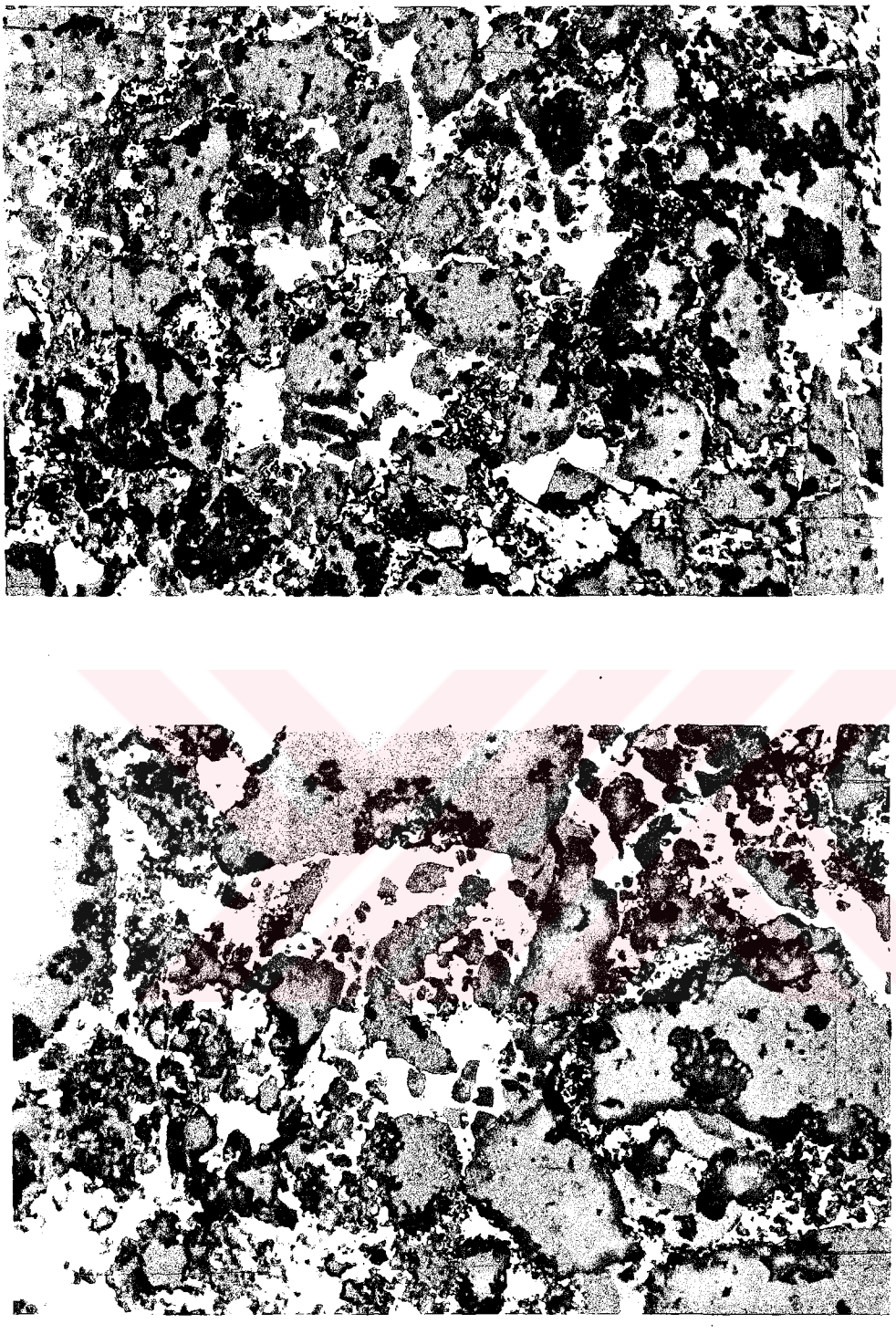

FIGURE: 4.15. AlN + 10% B4C sintered at 1600°C
Infiltration conditions: 1250°C, 400 torr
20 min

4.5. Mechanical Properties

Some rectangular bars have also been prepared for to measure 4- point bending strengths. Specimens were 4.8 mm thick, 6 mm wide and 50 mm long. The lower span was 38 mm and upper span was 20 mm. Tests were conducted with an Instron Universal Testing Instrument model 4505. Cross head speed was 0.1 mm/min. The highest strength was 195 MPa of the sample containing AlN + 50 wt% B_4C sintered at 1600°C and infiltrated under 50 Torr Ar, because of higher B_4C content. The strength of 4 %B_4C sintered at 1500°C was 53 MPa and 3 %B_4C sintered at the same temperature was 30 MPa. Since these results were obtained from one sample, the strength values may not represent the real behaviour. At least 10 samples necessary for a conclusion.

Macrohardness of the composites were determined with a Vickers indenter under 50 kg of load. The sample containing 50 wt% B_4C had an average hardness of 511 VH which is again the highest value. 5 measurements were done with each sample and average values are given in Table 4.4. As it is clear that, the hardness is decreasing with increasing argon pressure. Although the gas was purified before entering the system, it might have some impurities which causes oxidation of melted aluminum which prevents effective infiltration and also entrapment of argon gas in the pores of the ceramic preform may inhibit the intrusion of aluminum into pores which can also be the reason of lower hardness. The higher hardness of 10 % B_4C is possibly due to the higher content of B_4C.

TABLE: 4.4. Vickers macro hardness test results

Infiltration Atmosphere	AlN + 4% B_4C sintered at 1400°C infiltrated at 1250°C 20 minutes	AlN + 10% B_4C sintered at 1600°C infiltrated at 1250°C, 20 minutes
Vacuum	151.2	381
50 torr Ar	147.3	365
400 torr Ar	135.5	315

CONCLUSION

Wetting is an important factor for producing ceramic-metal composites by infiltration. In this study, B_4C was used to reduce the aluminum oxide film on AlN samples because aluminum oxide inhibits wetting of aluminum nitride with molted aluminum. B_4C reacts with aluminum oxide and yields to AlN and BN. For a full conversion the B_4C/Al_2O_3 ratio ws calculated to be 1.62. Therefore, for 1 and 2 % B_4C samples could not infiltrated because of the insufficient reduction.

Pore size and distribution effects the rate of infiltration. From porosimetry results, it was found that pore diameter decreases with increasing B_4C amount and increases with increasing sintering temperature. Since the particle size of B_4C is lower than that of AlN, B_4C particles are placing among AlN particles which might be the result of lower pore size.

Spesific areas of sintered products were measured, it was found that surface area is slightly decreasing with increasing sintering temperatures possibly due to sintering of particles.

The X ray analysis of infiltrated samples showed that intense Al peaks in the samples which have been fully infiltrated.

SEM studies of sintered powders, showed initialization of sintering at 1600°C. Therefore, sintering temperature of

1600°C provides somewhat continuous microstructure which is necessary for infiltration.

Hardness tests indicated that, as the content of B_4C increases, the hardness also increases. For vacuum infiltrations, aluminum metal intrude more freely into the pores. But under argon atmosphere, the pores are filled with gas which prevents aluminum intrusion. Therefore the hardness is decreasing with increasing gas pressure.

For further studies, sintering experiments can be done under argon atmospher in order to observe any weight change and how it affects infiltration. Investigation higher sintering temperatures can be recommended. And studies on BN / Al system may be helpful to understand the wetting behaviour of BN

REFERENCES

[1] DELANNAY, F., Review, The Wetting of Solids by Molten Metals and Its Relation to the Preparation of Metal-Matrix Composites, J.of Mater. Sci., 22, 1-16, (1987).

[2] TRUMPER, R.L., Metal-Matrix Composites - Applications and Prospects, Metals and Materials, Nov., 662-667, (1987).

[3] ERICH, D.L., Metal-Matrix Composites: Problems, Applications and Potential in the P/M Industry, The Int. J. of Powder Met., Vol:23, No:1, 45-54, (1987).

[4] LEWIS, C.F., The Exciting Promise of Metal-Matrix Composites, ME, May, 33-37, (1986).

[5] GEIGER, G., Progress Continues in Composite Technology, Am.Cer.Soc.Bull., Vol:70, No:2, 212-216 (1991).

[6] MROZ, C., Silicon Carbide-Whisker Preforms for Metal-Matrix Composites by Infiltration Processing, Am.Cer.Soc.Bull., Vol:72, No:9, 89-93, (1993).

[7] TOY, C., Processing of AlN/Al Composites, PhD Thesis, University Of Washington, (1991).

[8] MORTENSEN, A., Pressure-Infiltration Processing of Reinforced Aluminum, J.of Metals, Jan., 36-43, (1993).

[9] HALVERSON, D.C., Processing and Microstructural Characterization of B4C-Al Cermets, Ceram.Eng.Sci.Proc., 6, [7-8], 736-744, (1985).

[10] BANERJI, A., Role of Wettability in the Preparation of Metal-Matrix Composites (a Review), Metall, 38, 656-661, (1984).

[11] OH, S.Y., Particulate Wetting and Metal-Ceramic Interphase Phenomena, Ceram.Eng.Sci.Proc., 8, [7-8], 912-936 (1987).

[12] KINGERY, W.D., Metal-Ceramic Interactions: III Surface Tension and Wettability of Metal-Ceramic Systems, J.of Am.Cer.Soc., Vol:37, No:1, 18-23, (1954)

[13] EUSTATHOPOULOS, N., Structure and Chemistry of Metal/Ceramic Interfaces, in Designing Interfaces for Technological Applications: Ceramic-Ceramic, Ceramic-Metal Joining, Ed. by S.D.Peteves, Elsevier Applied Science Press, 197-215, (1988).

[14] EUSTATHOPOULOS, N., The Wetting of Carbon by Aluminum and Aluminum Alloys, J.of Mater.Sci., 9, 1233-1242, (1974).

[15] REED, J.S., Introduction to Principles of Ceramic Processing, John Wiley and Sons Publication, 22-25, (1988).

[16] RUHLE, M., Structure and Chemistry of Metal/Ceramic Interfaces, in Designing Interfaces for TechnologicalApplications: Ceramic-Cearmic, Ceramic-Metal Joining, Ed. by S.D. Peteves, Elsevier Applied Science Press, 145-195 (1988).

[17] SHALER, A.J., Theoretical Aspects of the Infiltration of Powder Metallurgy Products, Int. J. of Powder Met., 1, [1], 3-14, (1965).

[18] ASTHANA, R., On the Melt Infiltration of Copper Coated Silicon Carbide with an Aluminum Alloy, Composites Manufacturing, Vol:3, No:2, 119-123, (1992).

[19] GOETZEL, C.G., Infiltration Metals Handbook, 551-566

[20] LAVRENKO, V.A., Oxidation of Sintered Aluminum Nitride, Cer.Int., Vol:9, No:3, 80-82, (1983).

[21] KUROKAWA, Y., Development and Microstructural Characterization of High Thermal Conductivity Aluminum Nitride Ceramics, J.Am.Ceram.Soc., 71, [7], 588-594,(1988).

[22] YAN, H., Evolution of Carbon During Burnout and Sintering of Tape-Cast AlN, J.Amer. Ceram.Soc., 76, [1], 166-172, (1993).

[23] ENLOE, J.H., Microstructural Effects on the Thermal Conductivity of Polycrystalline AlN, J.Amer.Ceram.Soc., 74, [9], 2214-2219, (1991).

[24] TROCYNSKI, T.B., Effect of Additives on the Pressureless Sintering Of Aluminum Nitride between 1500-1800°C, J.Am.Ceram.Soc., 72 [8], 1488-1491, (1989).

[25] STERNITZKE, M., Growth of Oxide Layers on Thin Aluminum Nitride samples Measured by Electron Energy Loss Spectroscopy, J.Am.Ceram.Soc., 76, [9], 2289-2294, (1993).

[26] BLAKELY, K.A., Aluminum Nitride Ceramics, A Potential Material for Heat Management in Internal Combustion Engines, 3rd International Symposium on Ceramic Materials and Components for Engines, Las Vegas, NV, Edited by V.J. Tennery, Nov. 27-30, (1988).

[27] KOMEYA, K., Sintering of Aluminum Nitride: Particle Size Dependance of Sintering Kinetics, J. of Mater. Sci., 4, 1045-1050, (1969).

[28] LONG, G., Aluminum Nitride, a Refractory for Aluminum to 2000°C, J.of Am.Ceram.Soc., Vol:42, No:2, 53-59, (1959).

[29] LII, D.F., Mechanical Behavior of AlN/Al Composites, PhD Thesis, University of Washington, (1992).

[30] SURYANARAYANA, D., Oxidation kinetics of Aluminum Nitride, J.Am.Ceram.Soc., 73, [4], 1108-10, (1990).

[31] WEINER, A.W., Rapid Process for Manufacturing Aluminum Nitride Powder, J.Am.Ceram.Soc, 77, [1], 3-18, (1994).

[32] SHEPPARD, L.M., Aluminum Nitiride: A Versatile but Challenging Material, Am.Ceram.Soc.Bull., Vol:69, No:11, 1801-1812, (1990).

[33] SCHWETZ, K.A., Dense Molded Bodies of Polycrystalline Aluminum Nitride and Process for Preparation Without Use of Sintering Aids, U.S. Patent No: 4803183, Feb 7, (1989).

[34] KOMEYA, K., Sintered Bodies of Aluminum Nitride, U.S. Patent No: 4435513, March 6, (1984).

[35] SAKAI, T., Effect of Oxygen on Sintering of AlN, J. of Mater.Sci., 12, 1659-1665, (1977).

[36] LEFORT, P., Mechanism of AlN Formation Through the Carbothermal Reduction of Al_2O_3 in a Flowing N_2 Atmosphere, J.Am.Ceram.Soc., 76, [9], 2295-2299, (1993).

[37] RHEE, S.K., Wetting of Ceramics by Liquid Aluminum, J. of Amer.Ceram.Soc., Vol:53, No:7, 386-389, (1970).

[38] HALVERSON, D.C., Processing of Boron Carbide-Aluminum Composites, J.Am.Ceram.Soc.,72, [5], 775-780, (1989).

[39] WHITTEMORE, O.J., Pore Structure Characterization by Mercury Porosimetry, in Advances in Materials Characterization, Ed. by D.R. Rossington,Plenum Press, NY, 147-155, (1983).

[40] FUJII, H., Interfacial Reaction Wetting in the Boron Nitride/Molten Aluminum System, Acta. Metall., Vol:41, No:10, 2963-2971, (1993).

[41] HILLIG, W.B., Ceramic Matrix Composites by Means of Melt Infiltration, Ceram.Eng.Sci.Proc., 8, [7-8], 834-838, (1982).

CURRICULUM VITAE

Menderes Cìrakoglu was born Istanbul- Turkey in 1970. He graduated from Buyukcekmece High School in 1987 and attended to Istanbul Technical University, Faculty of Chemistry and Metallurgy in the same year. He received his B.S. degree in Metallurgical Engineering in 1991. He started graduate study in the same year at the Instìtute of science in Materials Science program.

He had a fellowship from United Nations Development Organization (UNIDO) for a short term training in University of Washington in 1993.